Vienna Conference Proceedings 2007, P. Moser et al.

A new reaction rate model for simulating the detonation process of the insensitive high explosives

X.M. Hu
National Key Laboratory of Computational Physics, Institute of Applied Physics and Computational Mathematics, Beijing 100088, China

Z.H. Wu
National Key Laboratory of Computational Physics, Institute of Applied Physics and Computational Mathematics, Beijing 100088, China

K. Yang
National Key Laboratory of Computational Physics, Institute of Applied Physics and Computational Mathematics, Beijing 100088, China

H. Pan
National Key Laboratory of Computational Physics, Institute of Applied Physics and Computational Mathematics, Beijing 100088, China

ABSTRACT: We build up a new reaction model by thinking of the excitation process and slow reaction in the detonation process of insensitive high explosives (IHE). This reaction model can be used in coarse mesh as compared with other reaction models. In the mesh of 50 cells per centimeter, the calculated results of the free surface velocity of copper flyer driven by JOB-9003 and JB-9014 are in accord with the experimental data. We also apply this model to calculate the process of IHE driving LiF. In the mesh of 50 cells per centimeter, the calculated result of the interface velocity between LiF and IHE accord with the experimental data. When the mesh size is smaller, the error between them is smaller. It indicates that this new model can describe the process of driven flyers by IHE in coarse mesh, and it can be widely used in practical works.

1. INTRODUCTION

Detonation of high explosives (HE) is very complicated. Generally, the chemical reaction process is not considered in practical works because computational resource is restricted. CJ (Chapman-Jouguet) theory is used to calculate the detonation process. Because the reaction zone of IHE is wide, the results calculated by CJ theory are not in accord with experimental results. Figure 1 shows the free surface velocities of Ta and Al flyer driven by PBX9502 calculated by CJ volume burn reaction model (Mader 1979) and experimental results.

It is obvious that the free surface velocities calculated by CJ volume do not accord with experimental results. It indicates that simulating the detonation process of IHE i.e. PBX9502 needs to consider the chemical reaction. As said before, the chemical reaction of HE is very complicated. There are many reaction processes in it, so it is hard to describe with the true reaction relation. The

phenomenological reaction models are used to calculate the detonation process of IHE i.e. JTF (Johnson 1985), Ignition & Growth (Lee 1980) and Hybrid (Tang 1993). The scale of the computational mesh of these models is very small, commonly above 200 cells per centimeter are needed (Tarver 1990). That would require a lot of computational time, so these models are hard to use in practical works.

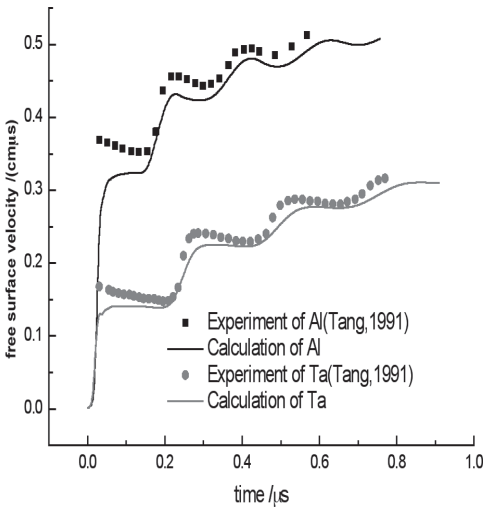

Fig.1 The free surface velocities of Al and Ta flyer driven by PBX9502 calculated by CJ volume and experimental results.

The flyer driven by HE is a very important problem in practical works, Pan (Pan 2007) established a new reaction model. Compared with other reaction models, the model is inspired in the excitation process and slow reaction in the detonation of HE (Tang 1993). It can simulate the work process of HE in the coarse mesh exactly. We used this model to calculate the free surface velocities driven by JOB-9003 and JB-9014, the calculated results are in accord with the experiments.

2. NEW REACTION MODEL

In practical works, the size of HE is commonly large. The work capacity of HE mainly depends on the stable detonation state, so the reaction model should describe the stable detonation state exactly. We established a new reaction model based on Hybrid reaction model, the detailed equations are:

$$\frac{\mathrm{d}\lambda_h}{\mathrm{d}t} = I\left(\frac{\rho}{\rho_0}-1\right)^{\alpha}\left(1-\lambda_h\right)^{\beta} \tag{1}$$

$$\frac{\mathrm{d}\lambda_b}{\mathrm{d}t} = \frac{1}{\tau_x}\left(\lambda_h-\lambda_b\right) \tag{2}$$

$$\frac{\mathrm{d}\lambda_s}{\mathrm{d}t} = \frac{1}{\tau_s}\left(\lambda_b-\lambda_s\right) \tag{3}$$

$$\lambda = \eta\lambda_h + \left(1-\eta-\psi\right)\lambda_b + \psi\lambda_s \tag{4}$$

Where λ is the mass fraction of the products of HE. *I*,α and β are constant. ρ_0 is initial density of HE. Subscripts h, b and s in turn stand for the hot spot, bulk reaction and slow reaction. η is the mass fraction of hot spot. ψ is the mass fraction of slow reaction. τ_x is the characteristic time of excitation process. τ_s is the characteristic time of slow reaction. Equation (1) refers to hot spot reaction. When I is small, the speed of hot spot reaction is slower and the peak value of pressure is higher. The mass fraction of hot spot is about 0.03. Equation (2) refers to excitation process. The main energy of HE is released in this process. The characteristic time τ_x controls the energy release speed. The value of τ_x is several nanoseconds. Equation (3) refers to slow reaction. When the mass fraction of slow reaction is larger and the characteristic time τ_s is longer, the energy release speed is slower. Commonly τ_s is tens of nanoseconds. The scale of ψ depends on the kind of HE. The scale of ψ of IHE is a little large and is about 0.15. This reaction model can describe the work process of HE and the speed between HE and inert material correctly. Fig 2 shows the $\lambda\sim \nu/\nu_0$ and $p\sim\nu/\nu_0$ of PBX9502.

Fig. 2 shows that the value of ν/ν_0 and p is equal to the CJ value at λ=1. It indicates that the pressure and density of the sonic point from new reaction model is according with CJ theory.

3. APPLICATION OF NEW REACTION MODEL

New reaction model is used to calculate JOB-9003 and JB-9014 driving 1mm copper flyer (YU 2006). Calculated results and experimental results are showed in Fig. 3 and Fig. 4.

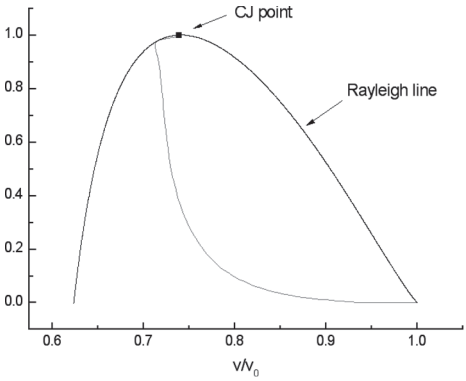

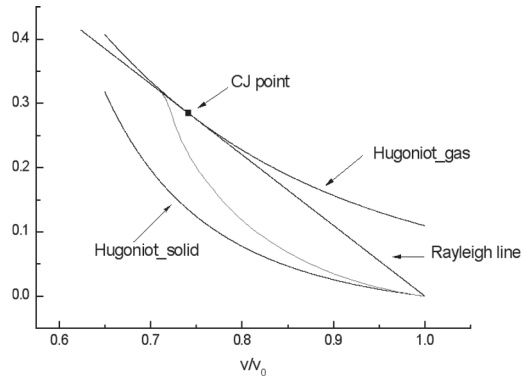

Fig. 2 ($\lambda \sim v/v_0$) and ($p \sim v/v_0$) of PBX9502

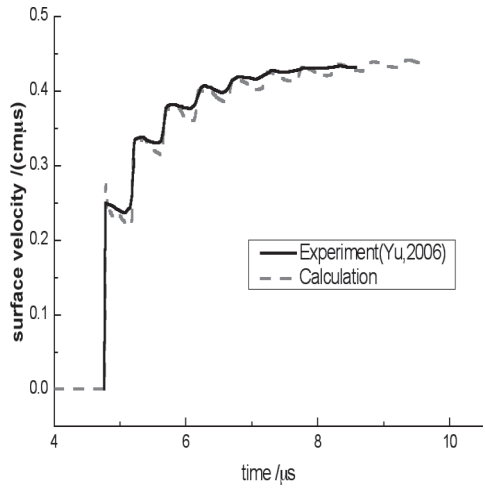

Fig. 3 The calculated free surface velocity of copper flyer driven by JOB-9003 and experimental results.

Fig. 3 and Fig. 4 show that the calculated results are close to experimental results. The difference between them is caused by the mechanical behavior of copper.

Generally, work process of HE is influenced by two main factors. One is the equation of state of HE. Another is the chemical reaction of HE. The calculation indicates that the free surface velocity of thin flyer depends on the chemical reaction of HE deeply. The first impacted velocity of free surface depends on the von-Neumann pressure of HE directly. The slow reaction of HE controls the energy released speed and influences the ultimate speed of flyer. Here the reaction model we were talking divides the chemical reaction into three parts, so it can describe the work process correctly. Of course, new reaction model also have some disadvantage. Because the new reaction model mainly concerns the steady detonation of HE, it could not describe the nonideal detonation very well i.e. deflagration to detonation transition (DDT). The new reaction model still needs some development in order to apply in the wide field.

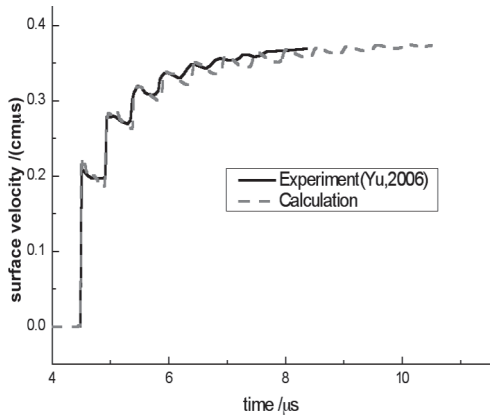

Fig. 4 The calculated free surface velocity of copper flyer driven by JB-9014 and experimental results

4. CONCLUSIONS

The new reaction model can describe the process of JOB-9003 and JB-9014 driving copper flyer correctly. That proves that the new reaction model can be used to simulate the work process of high explosive in the coarse mesh.

REFERENCES

Johnson, J.N., Tang P.K., Forest, C.A., 1985. Shock-wave initiation of heterogeneous reactive solids. *J. Appl. Phys.*, 1985, 57(9), 4323-4334.

Lee, E.L., & Tarver, C.M., 1980. Phenomenological model of shock initiation in heterogeneous explosives. *Phys. Fluids*, 1980, 23, 2362.

Mader, C.L., 1979. *Numerical Modeling of Detonation*. Berkely, California: University of California Press, 1979.

Pan, H., & Hu, X.M., 2007. A new reaction rate model for simulating the detonation process of the insensitive high explosives. *Explosion and Shock Waves*, 2007, 27(3), 236-239. (in Chinese).

Tang, P.K., 1993. A study of the role of homogeneous process in heterogeneous high explosives. *LA-UR-93-1557*, 1993.

Tang, P.K., 1991. Modeling hydrodynamic behaviors in detonation. *Propellants, Explosives, Pyrotechnics*, 1991, 16, 240-244.

Tarver, C.M., 1990. Modeling shock initiation and detonation divergence tests on TATB-based explosives. *Propellants, Explosives, Pyrotechnics*, 1990, 15, 132-142.

Yu, D.S., Zhao, F., Tan, D.W., et al. 2006. Experimental studies on detonation driving behavior of JOB-9003 and JB-9014 slab explosives. *Explosion and Shock Waves*, 2006, 26(2),140-144. (in Chinese)

Vienna Conference Proceedings 2007, P. Moser et al.

Adverse effects of dynamic shock waves on emulsion explosive sensitizers

M. Ahmad
Expancel, Eka Chemicals Inc (An Akzo Nobel Co.), Duluth, GA, USA

ABSTRACT: The adverse effects of dynamic pre-compression on typical emulsion type explosives sensitized either with glass or plastic microspheres are investigated. Each emulsion is evaluated for its comparative resistance to dynamic pre-compression by subjecting the explosive cartridges to dynamic shock waves of varying magnitude in an underwater environment. The rigid, relatively inflexible glass microspheres shatter once the applied dynamic shock wave exceeds their rated compressive strength and fails to detonate when initiated with the delay detonator. Test emulsion cartridges, incorporating plastic microspheres, also fail to detonate while under the direct influence of the dynamic shock wave, but recover as the dynamic shock wave pressure dissipates. The shocked cartridges incorporating plastic microspheres detonate when initiated with the delay detonator. The time interval, 0.003 – 0.004 seconds for the plastic microspheres recovery, and conditions for the product failure, together with the donor – receptor delay intervals for the sequential blasting are determined. The volume loss on recovered pre-shocked cartridges is also determined. The use of a free space sensitizer, which is more resistant to the adverse effects of dynamic pre-compression, results in the production of a more robust explosive product, for safer and environmentally cleaner blasting.

1. INTRODUCTION

When explosives detonate, they generate high pressure, compressive shock waves, which play an essential role in the rock breaking process. In most delay blasting applications, the relatively high pressures in these dynamic shock waves have the potential to impart significant damage to explosive charges in adjacent boreholes, which have not yet had a chance to detonate (Sumiya et al. 2003; Smith and Eck 2006). In the case of emulsion explosives incorporating glass or plastic microspheres as their primary sensitizing ingredients, the detrimental effects of these dynamic shock waves resulting from borehole to borehole interaction can lead to reduced performance or even complete failure of the explosives in adjacent bore holes. These situations are the subject of both safety and environmental concerns. The comparative abilities of these emulsion explosives to detonate after being subjected to dynamic shock waves of varying pressures were measured using a typical dynamic pre-compression test set-up. This test involved detonating a standard donor explosive charge underwater to generate a dynamic shock wave, which traveled outward through the water from the detonating explosive. The pressure in this shock wave dissipated as it propagated through the water. By suspending a cartridge of the test emulsion explosive (receptor charge) in the water at a known distance from the donor explosive charge, it was subjected to the compressive shock wave. By altering the separation distance between the donor and receptor charges, the magnitude of the

pressure in the shock wave affecting the emulsion receptor cartridge was varied. Also, by inserting a delay between the initiation of the donor explosive and receptor explosive charges (accomplished by the use of electric detonators and a sequential blasting machine), the detonability of the receptor explosive was evaluated before, during and after being subjected to the dynamic shock wave. As a result, the dynamic pre-compression test was used to examine the behavior of the various emulsion explosive products, by determining both if and how they were capable of recovering from the detrimental effects of a dynamic shock wave, once the pressure was allowed to dissipate.

The detrimental effects of dynamic shock wave pressures upon emulsion explosives sensitizers, as presented in this paper, were a part of Expancel®'s larger study, which examines the impact of the microsphere's particle density and size upon their sensitizing efficiency and heave energy in an emulsion explosive product. Therefore, it was necessary to review the nature of the two most common types of free space agents in more detail; i.e. glass microspheres and Expancel thermoplastic microspheres. The objective of this study is to evaluate the comparative performance of two different free-space agents (Expancel plastic microspheres and glass microspheres) when used as sensitizers in a basic detonator-sensitive emulsion explosive formulation, using the Dynamic Pre-compression / Relaxation Time Test.

The services of UTEC Corporation, which operates a commercial explosives testing laboratory in South-east Kansas, USA, were used to generate the test data presented in this study.

1.1 Glass microspheres

The glass microspheres used in this study to sensitize the emulsion explosives were hollow spheres constructed of borosilicate glass. A comparison of the physical properties of a typical low strength commercially available glass microsphere product and the Expancel plastic microsphere product are shown in Table 1. As compared to glass microspheres, plastic or polymeric microspheres, are more versatile and can be tailored by end users to the desired densities with particular particle size microspheres. They can be expanded in–situ in the explosives formulations or they can be pre-expanded using expansion units, powered by convectional heat or steam. Therefore, it is appropriate at this point to look at the nature of the plastic microspheres in a little more detail. Glass microspheres used in emulsion explosives as sensitizers are essentially borosilicate hollow spheres. The physical properties of the lowest density commercial grade glass microspheres and those of Expancel plastic microspheres are given in Table 1.

The plastic microspheres need to be in the expanded form in the explosives matrix to serve as sensitizers, generally in the 15 to 50 kg/m^3 density range. This includes ANFO prills, emulsions and water gels.

1.2 Expancel thermoplastic microspheres

These are essentially hollow spheres consisting of a thermoplastic outer shell encapsulating gaseous hydrocarbons as blowing agents. The particle size of the microspheres ranges from 10 – 32 microns diameter in their unexpanded form. On applying heat, the thermoplastic shell softens, the hydrocarbon gas pressure inside increases, and the microspheres will expand approximately four times in diameter compared to their original size; for example, a 20 micron size particle sphere expands to an 80 micron size sphere, as shown in Figure 1. This change in the sphere's particle size significantly affects the density of the microspheres, which

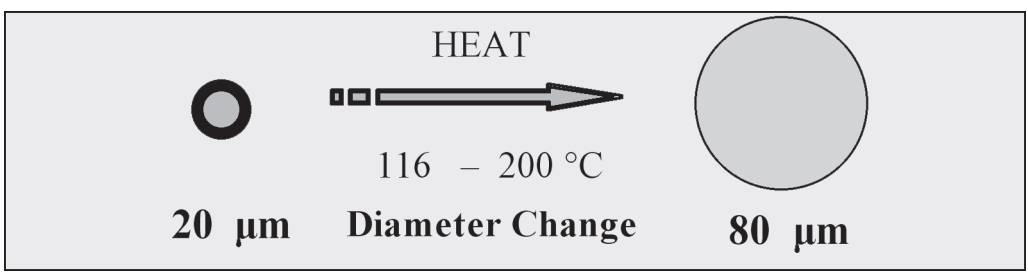

Figure 1a.

changes from a density of 1100 kg/m^3 for the unexpanded spheres to a density of 15 kg/m^3 for the expanded spheres. This results in about a 70 fold decrease in particle density of the plastic microspheres. To be an effective sensitizer in an explosive formulation, it is essential that the plastic microspheres be in their expanded state, which generally produces a particle density in the 15 to 50 kg/m^3 range.

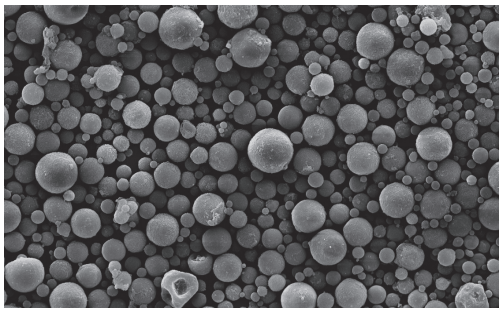

Figure 1b.

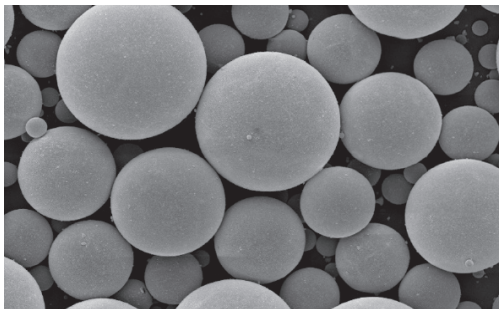

Figure 1c.

Figure 1. Diagram (a) and SEM photographs demonstrating changes in dimensions of Expancel® Microspheres on heating from UN – expanded (b) to expanded states (c).

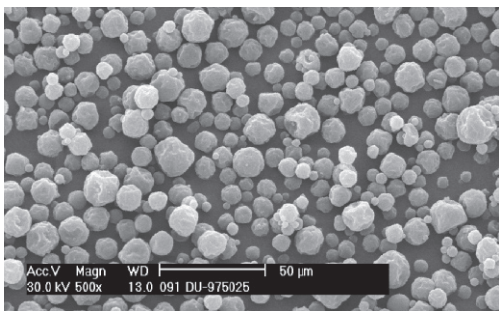

Figure 2a 10 Microns.

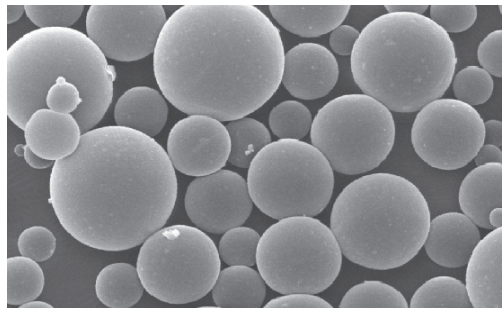

Figure 2b 40 Microns.

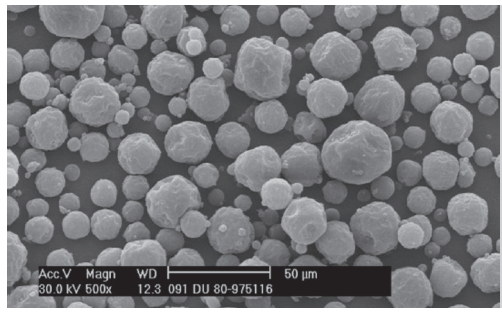

Figure 2c 18 Microns.

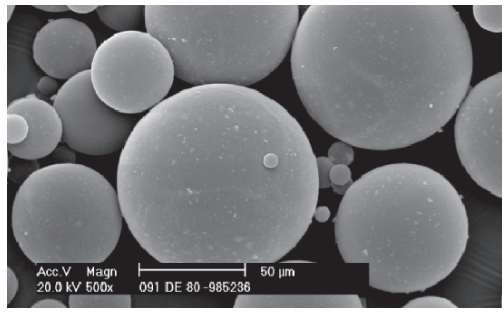

Figure 2d 80 Microns.

Figure 2. SEM photographs of plastic microspheres showing relationship between particle sizes, in unexpanded and expanded microspheres. Not shown: thirty micron size unexpanded microspheres change to 120 microns in diameter.

1.3 Elasticity - compression decompression

Due to the nature of their materials of construction, the shells of plastic microspheres are elastic. Therefore, when subjected to a sufficient pressure load, they have a tendency to buckle or shrink in size, due to the compression of the gas inside the

spheres. By the same token, when the pressure load is removed, the microspheres rebound back to their original shape and size.

2. TESTS AND TEST MATERIALS

The emulsion explosive products used in the pre-compression tests were prepared in the UTEC laboratory's explosive pilot plant, using the free space agents supplied by Expancel. The detonator sensitive explosives consisted of a typical dual salt (ammonium nitrate and sodium nitrate) oxidizer solution, which was emulsified with an organic fuel solution (blend of wax, mineral oil and PIBSA surfactant). The final emulsion explosive product had water content in the 11 percent range. Each free-space sensitizer was incorporated in the hot emulsion matrix to achieve a final emulsion density in the 1050 -1100 kg/m^3 range. The properties of the free-space agents are listed in Table I. The two sensitized emulsion test mixes were made in the UTEC Lab's pilot plant, using a hand mixing technique to blend the various free space agents into the hot matrix emulsion. The ingredient composition for the two emulsion test batches are listed in Table 2. Once produced, the sensitized emulsion mixes were packaged into 50.8 mm (2-inch) diameter poly chub cartridges for the required series of detonation testing.

Brief descriptions of the various comparative tests are given in the following sections.

2.1 Pre-compression / relaxation time tests

This test involved subjecting the sensitized emulsion explosive mixes to dynamic pressures, which are commonly encountered when bore-holes are sequentially fired in a delayed shot pattern (Hustrulid 1999). Due to the elastic nature of the Expancel microspheres, they compress and do not readily break when subjected to the dynamic compressive shock wave. When compressed, the sensitizing efficiency of the plastic microspheres is greatly reduced, even to the point that the explosive product is no longer detonable. However, once the shock wave has passed and the pressure dissipated, the elasticity of the plastic microspheres allows them to regain their original shape/volume, and once again become effective emulsion sensitizers. Glass microspheres, on the other hand, can be broken when subjected to a dynamic compressive shock wave that exceeds their rated crush strength.

Both pre-compression test methods used in this study contained the same basic donor/receptor charge set-up. After a varying delay period, the sensitized emulsion cartridges (50.8 mm diameter poly chub cartridges) were initiated with a standard electric detonator, after being subjected to the compressive shock wave generated by a donor explosive charge (DYNO NOBEL Spartan 450, one-pound cast booster). Commercially available electric detonators (zero delay) were used to initiate both the donor and receptor charges and a two channel sequential blasting machine was used to provide the desired delay period between the firing of the two charges. The detonation of each receptor emulsion test cartridge was monitored using the VOD (Velocity Of Detonation) test method. Both the donor and receptor charges were suspended in the Lab's main water-pit, at a constant depth of 3.048 meters. These detonation tests were conducted at an ambient temperature in the 20-25°C range. A diagram of the test set up is given in Figure 3.

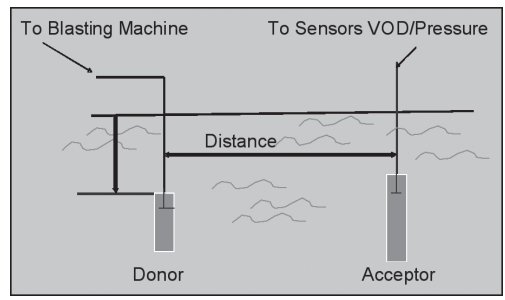

Figure 3. Under water dynamic pre compression / decompression test set-up, where the donor-to-acceptor charge separation distance is varied to increase or decrease the pressure in the shock wave as it passes over the acceptor charge.

In order to quantify the magnitude of the shock wave pressure to which the test emulsion cartridges were being subjected, a pressure versus distance profile for the one pound cast booster donor charge was generated. This shock wave pressure profile is given in the attached Figure 4. Both the donor and receptor charges were suspended under water at a constant charge depth of 3.048 meters, with the variable donor-to-receptor separation distance being altered in 0.3048 meter increments. Both explosive charges were initiated with a zero delay electric detonator. A 0.025 seconds (25-milliseconds) delay between the initiation of the donor and

receptor explosive charges was provided by a dual channel blasting machine.

Due to the compressibility of the Expancel microspheres, it was necessary to insure that the emulsion cartridges sensitized with these plastic microspheres were being initiated while under the direct effect of the shock wave. Therefore, it was necessary to conduct several preliminary tests to measure the propagation speed of the shock wave in water. This was conducted using a simple oscilloscope / pressure transducer set-up, which measured the time interval from the firing of the booster charge to the time when the shock wave / pressure pulse arrived at the pressure transducer, which was located at a stationary distance of 3.048 meters from the booster charge. The results of these tests are given in Figure 4

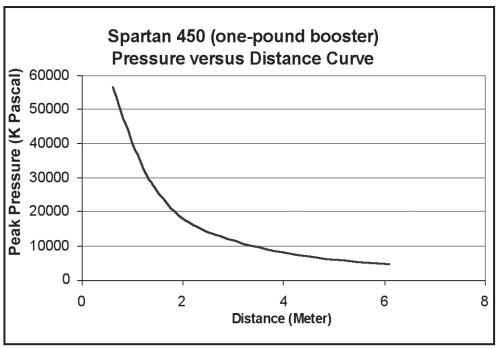

Figure 4a

Product	Shock Wave Travel Time Seconds	Measured Peak Pressure kPa
Spartan 450 cast booster	0.0020	10,313
	0.0020	11,478
	0.0020	10,389
	0.0019	10,968
	0.0020	11,106
Average (s)	**0.002**	**10,850**

Figure 4b

Figure 4. (a) Spartan 450 g booster blast pressure (kPa) versus distance (meters) (b) showing Peak pressure and shock travel time (seconds).

Raw Materials: The following free space sensitizers were used in these tests.

Table1. Free space sensitizer and Matrix Emulsion specifications.

Material	Particle Size (Average μm)	Density kg/m^3
Expancel Plastic microspheres 009 DET 80 d15	60 – 90	15.0 Elastic and compressible
Glass microspheres	65 – 85	12.5 Rigid Crush strength of 1,723 kPa
Matrix Emulsion	N/A	1380 cup density at 80°C

Sensitizer Composition:

Table 2. Ingredient weight percent composition and final density of sensitized emulsions.

Ingredient	Formula 1	Formula 2
Matrix Emulsion wt Percent	97.3	99.66
Glass Microspheres wt Percent	2.7	0
Expancel 009 DET d15 wt Percent	0	0.34
Sensitized Emulsion Density kg/m^3	1090 – 1100	1070 – 1080

3. PRECOMPRESSION /RELAXATION TIME TEST DATA

3.1 Formula 1 glass microspheres sensitized emulsion

In this test, the Formula 1 emulsion cartridges were suspended in the water at a constant donor-to-receptor separation distance of 3.048 meters. At this distance, the pressure in the shock wave as it impacted the emulsion cartridge was measured to be in the 10,850 KPa, which was more than enough pressure to break the glass microspheres. Under these test conditions, the Formula 1 emulsion cartridges failed to detonate after being subjected to the compressive shock wave. The results are shown in Table 3.

Table 3. Pre-compression / relaxation time test data for Formula 1 containing glass microspheres at 3.048 meters separation distance from Spartan 450 donor charge. * Low order detonation, below 2800 m/s considered to be failed.

Pre-Compression/Relaxation Time Test Data for Formula 1 at 3.6576 meters separation distance from Spartan 450 donor charge successfully detonated for all the delay times shown in Table 3.

3.2 Shocked cartridge densities

To get some understanding of the level of glass microsphere loss on dynamic shock wave impact at different donor to receptor separation distances from the booster charge, glass microsphere sensitized emulsions were shocked and recovered for density measurements. The results are given in Table 4. A density of 1190 kg/m^3 was measured on a recovered shocked cartridge of the Formula 1, which had been shocked at the 3.6576 meters separation distance, indicating that a certain percentage of the glass microspheres had been broken when subjected to the pre-compressive shock wave (glass microspheres had suffered a volume loss equal to about 35% of their original volume).

3.3 Formula 2 plastic microsphere sensitized emulsion products

The dynamic pre-compression test for the emulsion sensitized with Expancel microspheres was carried out only with a donor-acceptor distance of 3.048 meters. In this test, both donor and receptor charges were suspended in water at a constant depth and at a constant separation distance of 3.048 meters. It was experimentally determined that the speed of the shock wave, as it propagated outwards from the detonating donor charge, was such that it required about 0.002 seconds to reach the emulsion receptor cartridge located 3.048 meters away. In order to evaluate the emulsion cartridge's performance before, during and after the direct influence of the shock wave, varying delay periods in the 0.002 to 0.100 s range were inserted between the instant (zero delay) detonators used to initiate the donor and receptor charges. An average pressure in the 10,685 -11,030 kPa range was measured in the shock wave at the 3.048 meter distance.

Test data in Table 5 shows that the plastic microsphere sensitized emulsions recover from the effects of the dynamic shock wave of about 10,685 KPa in total time of approximately 0.006 seconds, and remain detonable for at least 0.100 second after being exposed to the compressive force of the shock wave. However, since it takes approximately 0.002 seconds for the shock wave to travel from the Spartan 450 Booster to the donor target at a 3.048 meter separation distance, the recovery time for the Expancel microspheres in this experiment is determined to be approximately 0.004 seconds. A density of 1110 kg/m^3 was measured on a

Table 3. Pre-compression / relaxation time test data for Formula 1 containing glass microspheres at 3.048 meters separation distance from Spartan 450 donor charge. * Low order detonation, below 2800 m/s considered to be failed.

Product	Delay Time Seconds	Result/VOD m/s
Formula 1 (Glass microspheres)	0.002	Failed
	0.004	Failed
	0.006	LOD*
	0.010	Failed
	0.100	Failed

Table 4. Densities of recovered shocked cartridges of the Formula 1 product, shocked at varying distances, and corresponding volume loss of the glass microspheres.

Distance Separation (m)	2.438	3.048	3.6576	4.2672
Shock Wave Pressure (kPa)	13,788	10,685	8,617	6,894
Density (shocked) Cartridge kg/m^3	1380	1310	1190	1140
Percent Volume Loss	100	78	35	14

Table 5. Pre-Compression/Relaxation Time Test Data For plastic microspheres, Formula 2 Product at 3.048 meters separation distance from Spartan 450 donor charge, generating dynamic shock wave pressure equivalent to 10,685 kPa.

Product : Formula 2	Delay Time seconds	Result/VOD (m/s)
Plastic Microspheres (Expancel 009 DET 80 d15)	0.003	Fail, partial charge recovered
	0.003	Fail, partial charge recovered
	0.005	Fail, partial charge recovered
	0.006	Detonated, VOD = 5,907 m/s
	0.006	Detonated, Target shot off
	0.007	Detonated, VOD = 4,996 m/s
	0.010	Detonated, VOD = 5,219 m/s
	0.015	Detonated, VOD = 5,298 m/s
	0.100	Detonated, VOD = 5,861 m/s

recovered cartridge of the plastic microspheres sensitized emulsions product, previously shocked at the 3.048 meters separation distance.

4. DISCUSSION

Pre-compression/relaxation time test data for glass microspheres sensitized emulsion, as Table 3 shows; at 3.048 meters donor-receptor separation distance the compressive shock wave pressure, 10,685 kPa, impacting the emulsion cartridge was high enough to break a sufficient amount of the glass microspheres. The resulting desensitized emulsion cartridge failed to be initiated with the electric detonator. At a separation of 3.657 meters, the glass microspheres emulsion successfully detonated for all the time. Additionally, to get some understanding of the level of glass microsphere loss on dynamic shock wave impact, glass microspheres sensitized emulsions were shocked at different donor to receptor separation distances and recovered for density measurements. The glass volume loss in these cartridges, as shown in Table 4 is between 14 percent and 100 percent as the distances are varied from 4.2672 meters to 2.438 meters.

In the case of the Expancel plastic microsphere (Formula 2) sensitized emulsion mixes, a constant separation distance of 3.048 meters was maintained between the donor and receptor charges. At this separation distance, the emulsion receptor cartridge was being subjected to a maximum shock wave pressure in the 10,685 -11,030 kPa range, arriving in the vicinity of the emulsion cartridge about 0.002 seconds after the detonation of the cast booster donor charge. A delay period was applied to the instant (zero delay) electric detonators used to initiate both the donor and receptor explosive charges. Once a delay period was established where the emulsion charge failed to detonate, i.e. plastic microspheres under compression, then additional shots were made with increasingly longer delay periods between the firing of the donor and receptor charges. The delay time was increased in 0.001 second (1 millisecond) increments, until the emulsion charge was once again able to detonate. The plastic microspheres 'bounced back' from the compressive effect of the high pressure shock wave. The recovery time of the

plastic microsphere sensitized emulsion explosive products was determined to be at around 0.004 seconds. This is based on the delay time, at which the emulsion cartridge was once again detonable, and subtracting the 0.002 second time interval that was required for the shock wave to travel the 3.048 meters separation distance between the donor and receptor explosive charges. The plastic microspheres remained intact as evidenced by the residual density of 1100 kg/m^3 measured on a recovered cartridge of the plastic microspheres sensitized emulsion product, previously shocked at the 3.048 meters separation distance.

5. CONCLUSION

Emulsion cartridges incorporating glass microspheres as sensitizers reduce their volume due to breakage when subjected to dynamic shock waves exceeding the crush strength of the glass microspheres. At the 3.048 meter donor–receptor separation distance corresponding to 10,720 kPa shock pressure, the volume loss is approximately 78 percent, and the cartridges do not detonate with the electric detonator after the time delays employed between 0.002 seconds and 0.100 seconds. Under the same donor-receptor separation distances the shocked cartridges incorporating plastic microspheres as sensitizers, compress, and recover after approximately 0.004 seconds, after which the cartridges detonate with electric detonator with the time delays between 0.006 to 0.100 seconds. The density measurements on a recovered cartridge of the plastic microsphere sensitized emulsions product, previously shocked at the 3.048 meters separation distance show no loss in volume of the plastic microspheres. The plastic microspheres recovered from the effects of dynamic shock once the affecting pressure had been allowed to dissipate. The use of more resilient explosives products, which are better equipped to withstand or overcome the desensitizing effects of dynamic pre-compression, should result in safer and more efficient blasting operations.

REFERENCES

Hustrulid, W. 1999. Drilling Patterns and Hole Sequencing. *Blasting Principles for Open Pit Mining*, Vol. 1, 144 – 149 & 254 – 257. Rotterdam: Balkema.

Smith, C. & Eck, G. 2006. Detonator Malfunction – Sensitizer Effects. Proc. of the 32nd *Annual Conference on Explosives and Blasting Technique. International Society of Explosives Engineer, January 29 – February 1*, 2006. Dallas, Tx.

Sumiya, F.Y., Hirosaki & Kato, Y. 2003. Influence of the pressure wave propagating in compressed explosives on detonator. Proc. of EFEE Second World Conference on Explosives and Blasting *Technique, 10 -12 September 2003*, Czech Republic.

Vienna Conference Proceedings 2007, P. Moser et al.

Large scale testing of ammonium nitrate

E.C. Nygaard
Yara Industrial, Technology Centre, Porsgrunn, Norway

ABSTRACT: During the last years, ammonium nitrate (AN) has been involved in several accidents worldwide. These have caused an increased focus on AN and resulted in revised Yara standards, new international standards for transportation and stricter regulations from national authorities in many countries.

In 2006 Yara decided to launch a new test program with focus on various grades of Porous AN (TAN). Therefore a study on handling of ammonium nitrate was initiated. The aim of this study was to verify safety aspects and to optimise storage layout for technical ammonium nitrate (TAN). To do this we had to determine guidelines for separation distances between stacks of big bags and between silos and to calculate the maximum storage amount based on the maximum allowable overpressure for facilities, storages and silos.

In this study, tube tests were performed to measure the blast waves from detonation of TAN. The data from the tube tests were used to calculate the TNT equivalence of the TAN.

Gap tests were performed to determine the critical gap length between an ANFO donor and a TAN acceptor. The results of the gap tests were used in simulations to determine the critical separation distance between stacks of big bags and between storage silos.

1. INTRODUCTION

Ammonium nitrate (AN) is chemically speaking a simple salt with complex, hazardous properties. The specific hazardous properties are determined by physical properties of the material (particle size, porosity and density), chemical properties (purity, stabilisers and moisture), environmental factors (confinement and compatibility with other materials) and conditions such as temperature and pressure. Generally speaking, the risk associated with ammonium nitrate in production, transport and storage is low.

Under severe conditions, all types of AN are able to detonate. Despite the low probability for the occurrence of a detonation under practical (including accidental) conditions, the hazards with AN should be understood due to the severe effects of such an event. The detonation properties (initiation sensitivity, detonation velocity and effect) of AN depend on many factors. With respect to safety in storage and transport however, the 'sensitivity' of the material towards initiation is the most important parameter in controlling the hazards.

The 'sensitivity' of AN is determined by the critical diameter (a detonation cannot be sustained below the critical diameter) and the response

Table 1. Characteristics of TAN samples tested.

	Bulk density (1 l cylinder) (kg/l)	Oil absorption (%)	Average loading density, tube test (kg/l)	Average loading density, GAP test (kg/l)
TAN 1	0.81	7.6	0.84	0.83
TAN 2	0.72	12.1	0.72	0.73
TAN 3	0.79	10.7	0.81	0.80

to thermal and shock stimuli. From both own experience and literature data, it appears that one of the main factors affecting the detonability of AN (critical diameter and minimum booster) is bulk density. From a study performed by Bauer et al. (1982) in the 70s it can be concluded that the critical diameter of high density AN (>0.9 kg/l) is in the order of metres.

In 2005 to improve understanding of safety properties of AN, the European Fertilizer Manufacturers Association (EFMA), Brussels, Belgium, initiated a study on safety aspects related to the sensitivity to detonation of ammonium nitrate (AN) and AN based fertilisers. The Dutch research institute TNO in the Netherlands was contracted to perform the work. The main aim of the study was to provide the industry with further knowledge and understanding on AN safety and to provide a sound basis for the guidelines for storage, distribution and use of AN and AN-based products in Europe. Since the focus in the EFMA/TNO study were on high-density fertilisers, Yara decided to launch a new test program in 2006 with focus on various grades of Porous AN (TAN). TNO was contracted to perform the study.

During our work to verify our own internal standards for porous ammonium nitrate (TAN) we found that the information available from previous studies was both confusing and non-conclusive. In many studies the TAN used had not been properly defined and therefore the interpretations of the previous results were difficult.

2. TESTS AND RESULTS

2.1 Test material

In all tests performed, three types of TAN were used (Table 1).

2.2 Tube tests: Determination of TNT equivalence

The main purpose of the tube tests was to determine the TNT equivalence of the test materials. The tests were performed at a test site close to Älvdalen, Sweden, in close cooperation with FOI (Swedish Defence Research Agency).

Cylindrical polymer-ceramic tubes were used. The diameter of the tube was 1.16 m and the height 4.0 m, which gives an L/D ~ 3.4. From experience it is known that the critical diameter of TAN is far below a diameter of 1.16 m. The wall thickness of the tubes was 3 cm. The influence of the diameter of the tube is more significant than the increase in confinement caused by the wall of the tube.

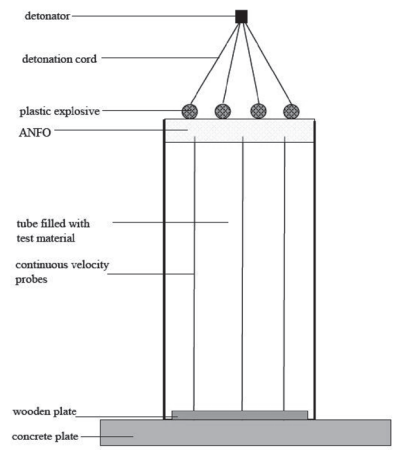

Figure 1. Set-up of tube test (please observe that three rings of plastic explosive was used but only two are shown in the illustration).

By simulations we found that a flat shock wave was obtained when three rings of plastic explosives initiates a 30 cm thick layer of ANFO (booster). The rings were initiated 'at the same time' at several

places by applying a detonator and 16 detonating cords of equal length.

For the measurements of the detonation velocity (VOD), three continuous velocity probes (resistance wires) were inserted in the tube before it was filled with TAN. The top of the tube was filled with an ANFO layer of 30 cm with three rings of plastic explosives slightly buried at the top of the ANFO.

For each test the blast was measured in terms of peak overpressures at three distances from the tube in two directions (south (S) and west (W)), with pencils at 40, 80 and 160 m. The blast was measured with PCB Piezotronics, model 137A23/137/M30 with a frequency of 100 kHz. The height of the blast pencils was 1.6 m from the ground.

From VOD recordings and pressure measurements it can be concluded that detonation occurred in all three tube tests. All VOD plots showed a straight line over the entire length of the column. The measured VODs were all close to ideal calculated values obtained by the thermodynamic programme Cheetah.

The TNT equivalence was determined using the TNT model for damage calculations. The TNT model is based on the cube root law of Hopkinson (Baker et al. 1983) that states that when two charges of the same explosive and geometry but of different size are detonated in the same atmosphere, self-similar shock waves are produced at the same scaled distance. The scaled distance Z [m/kg$^{1/3}$] is defined as:

$$Z = \frac{r}{W^{1/3}} \qquad (1)$$

where r is the distance [m] and W the charge mass [kg]. The TNT explosion model gives peak side-on overpressure, P, as a function of the scaled distance, Z. Hence, by using the TNT model; the side-on overpressure at any distance for a given amount of TNT can be calculated. The TNT model can also be used to predict the damage from other exploding materials if the explosive strength of these materials can be translated into an equivalent amount of TNT. Subsequently, this amount of TNT is used to determine the blast load on the surrounding and the resulting damage.

The peak pressure plots are more or less equal for both directions (S and W). The TNT equivalence is more or less equal for the three materials; and the fluctuations are small. The values of the TNT equivalences are more or less in agreement with the theoretical values, based on the energy release. The results showed that the TNT equivalence was decreasing with an increasing distance from the detonation. For one of the samples the TNT equivalence was found to be 0.60 at a distance of 40 m and 0.39 at a distance of 160 m. The TNT equivalences in the present study are relatively high compared to the values calculated from incidents (10 – 20 % TNT equivalence). In the interpretation of the equivalence value obtained in these tests it must be kept in mind that the tests were fully optimised with respect to configuration and very strong initiation source was used.

2.3 GAP tests

The purpose of gap tests was to determine the sensitivity of the materials (initiation pressure). In these tests the critical separation distance between a donor and an acceptor was determined, i.e., the minimum distance at which a sympathetic detonation between donor and acceptor is no longer possible.

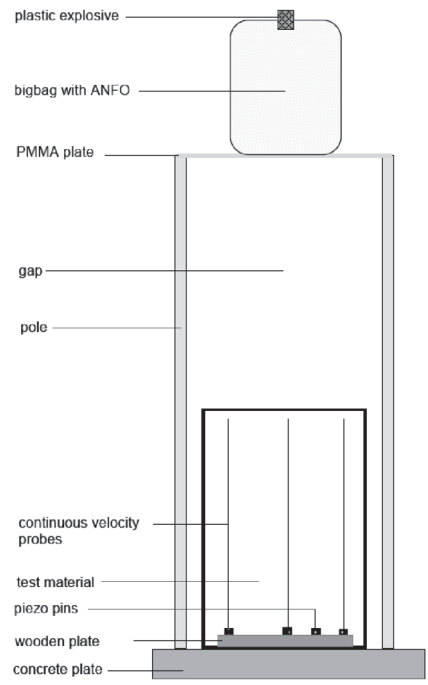

Figure 2. Set-up of the GAP test.

For the determination of the sensitivity of the material, vertically placed cylindrical polymer-ceramic tubes were used. The diameter of the tube was 116 cm, L/D ~ 1.7 and wall thickness 3 cm. The tube was filled with the test material, to act as the acceptor.

For the measurements of detonation velocity three continuous velocity probes (resistance wires) were used. The length of the probes was equal to the length of the tube. Before the tube was placed on a concrete plate on the ground, a wooden plate was placed in the bottom (see Figure 2) to fix the resistance wires. In these tests 350 kg of ANFO (in a big bag) was used as donor material, because the detonation pressure of ANFO is above the initiation pressure of ammonium nitrate and ANFO is easy to apply. The ANFO was initiated with 1 kg of plastic explosives. The diameter of the donor should be more or less the same as the diameter of the acceptor. The ANFO donor was placed on top of a wooden construction above a tube filled with test material (acceptor) (see Figure 2 and Figure 3). The big bag of ANFO was placed on a 10 mm thick PMMA plate. By changing the length of the 'legs', the distance (gap) between the donor and acceptor could be varied. In these tests, the distance between donor and acceptor was varied between 1.5 and 3.5 m.

The tests showed that the critical separation distances varied between 2.0 and 3.0 m, depending on which TAN was used.

Figure 3. Gap test.

2.4 Simulations

In the gap test the critical separation distance between an ANFO donor and a TAN acceptor was determined. From the results of the gap tests the critical initiation pressure of the three TAN grades and the critical separation distances were determined with simulations. In paragraph 2.4.1 the theory of the simulations is given. The results of simulations for the critical initiation pressure are described in paragraph 2.4.2. From the results of the critical initiation pressure the critical separation distance for bigbags in practical situations (storage) was determined and the results are given in paragraph

Note that in the gap tests ANFO is used as donor and TAN acts as the acceptor, while in the practical situation TAN is the donor and the acceptor. A detonation of TAN gives another pressure than the detonation of ANFO and therefore the critical separation distance in the practical situation is different from the gap tests.

2.4.1 Separation distances and maximum storage amount

In literature, several tables with separation distances for AN can be found. Most of these tables seem to originate from the American Table of Distances (NFPA, 1968) that was issued in the 60s. Originally, the table was issued for high explosives, but with given correction factors, it can also be used for AN. However, as described in notes to this table, ammonium nitrate, by itself, is not considered to be a donor when applying this table. Ammonium nitrate, ammonium nitrate- fuel oil or combinations thereof are acceptors. If stores of ammonium nitrate are located within the sympathetic detonation distance of explosives or blasting agents, one-half the mass of the ammonium nitrate is to be included in the mass of the donor.

The separation distances are given as a function of the mass of the donor (the critical separation distance is virtually independent of the mass of the acceptor). The relation between mass and separation distance is nearly the same as the relation that follows from the so-called pyrotechnical equation (Medard 1989). According to this equation, the critical separation distance is proportional to the cube root of the mass of the donor. The background of the pyrotechnical equation is the scaled distance approach for damage calculations as used in the TNT equivalence model. The scaled distance approach is based on a 'simple' configuration of the

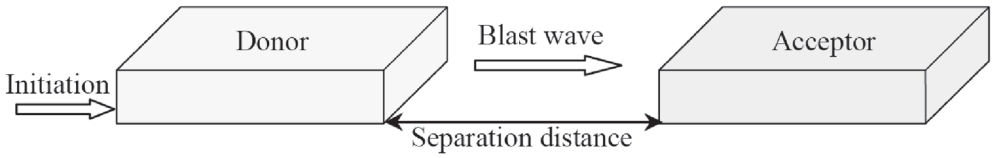

Figure 4. A schematic basic overview of the model used to calculate separation distances.

donor in the form of a hemisphere. Furthermore, the size of the hemisphere is considered small compared to the distance, at which the effects are considered. This means that only the mass of the donor is considered, not its size. The fact that the configuration of the donor is not included in the equation (therefore also not in the ATD) and that the proportionality factor is not well determined for ammonium nitrate, is a real disadvantage in the application of the equation (or the ATD). For many practical situations, unrealistic separation distances therefore can be found.

To overcome the disadvantages of the ATD and the pyrotechnical equation, a new approach towards the problem of critical separation distances was developed at TNO. The model is more complex but leads to smaller (more realistic) separation distances as it takes all relevant parameters, related to sympathetic detonations, into account. These parameters are strength of detonation of donor, place of initiation and configuration of donor, orientation between donor and acceptor and initiation sensitivity of acceptor. A schematic overview of the model is presented in the figure below (Figure 4).

The first step in the model is the determination of the shock wave from a detonation of the donor. A conservative estimation of the shock wave is obtained if a conservative place of initiation is assumed (in a plane at the far end of the acceptor) and if the detonation strength of the donor is based on theoretical detonation parameters (ideal detonation). Note that the blast (shock wave) of the donor can be determined for any given configuration of this donor. In the second step, the blast load on the acceptor is calculated as a function of distance. To obtain a conservative result, the load is evaluated at the explosive interface near the ground level and at half depth. The blast load is compared with the initiation sensitivity of the acceptor to determine whether or not an initiation, and thus a sympathetic detonation can take place.

The critical separation distance strongly depends on the initiation sensitivity of the AN. The approach above applies to material as produced. It is important to note, however, that the required separation distance significantly increases if the material becomes sensitised (for example by moisture, temperature or aging). This does not have to be a bulk effect; formation of a sensitised layer of material on the outside of a pile or stack might already be sufficient to affect the separation distance. Whether or not this effect has to be taken into account depends on many factors and on the scenarios that are taken into account.

2.4.2 Critical initiation pressure

In gap tests the critical separation distance between an ANFO donor and a TAN acceptor was determined. This was used to calculate critical initiation pressure for the three grades of TAN that were tested. To determine the critical initiation pressure simulations were performed with the computer programme Autodyn. The donor in the simulations was a cylinder with a diameter of 1.00 m and height of 0.52 m. The donor material was 350 kg ANFO with a density of 850 kg/m^3. The acceptor was a cylinder with a diameter of 1.20 m and a height of 2.40 m. Simulations were performed for all three types of TAN as acceptor material. These values where then used in simulations to calculate the critical separation distances between stacks. Note that in the gap tests ANFO was used as donor and TAN acted as the acceptor, while in the practical situation TAN is both donor and acceptor. A detonation of TAN gives another pressure than the detonation of ANFO and therefore the critical separation distance in the practical situation is different from the gap tests.

From these simulations the critical initiation pressures were calculated.

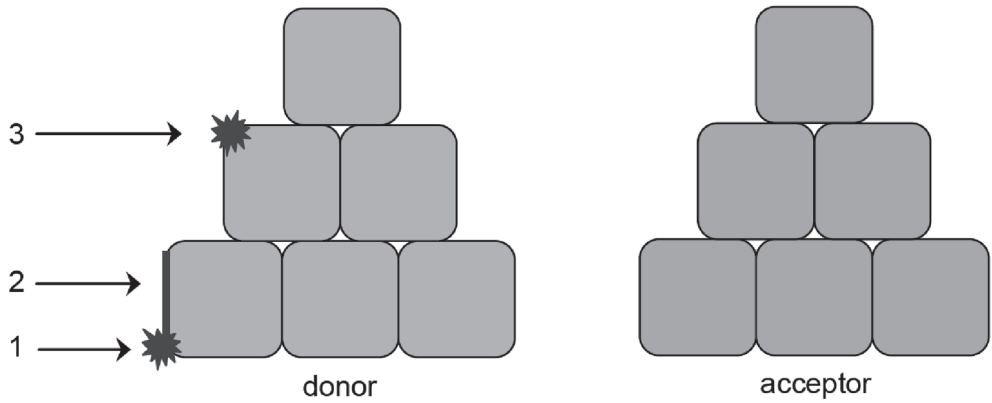

Figure 5. Configuration for simulations with donor and acceptor stacks. Donor and acceptor are the same material.

2.4.3 Critical separation distances

On the basis of the values of critical initiation pressure, simulations were performed to determine critical separation distances between stacks of big bags filled with TAN. In this paper, results from simulations with one TAN grade are shown.

The simulations were performed for a stack with three layers of big bags. In the first set of simulations, the bottom layer contained 12 big bags, the middle layer 11 big bags and the upper layer 10 big bags. The length of the row in the practical situation is equal to the diameter of the row, so the bottom layer contained 12 x 12 big bags. In the simulations the propagation of the detonation was assumed to be in the direction of the acceptor (conservative), opposite to the length of the pile. The big bags in the simulations contained 1000 kg material and had a diameter of 110 cm and a height of 120 cm. The loose bulk density of the TAN is 0.73 kg/l (measured in the tube and gap tests). The material density of the donor material used in this simulation was 0.69 kg/l to take into account the space between the big bags to get the right amount of material.

The strength of the blast wave was determined by the total energy available in the donor and is therefore a function of average effective density of the donor explosive. In the acceptor stack the true density of the material of 0.73 kg/l was used since the amplitude of the (reflected) blast wave at the acceptor is a function of the shock impedance of the acceptor material. In the simulations the donor stack was initiated on the site opposite to the acceptor (see Figure 5) and the detonation propagated through the donor stack in the direction of the acceptor. From a previous study it was concluded that the way of initiation of the donor stack affects the critical separation distance between stacks. Therefore simulations were performed in which three different initiation points were used (See Figure 5):

- Point initiation at the bottom of the bottom layer
- Surface initiation at the bottom layer (height of 1 big bag)
- Point initiation at the top of the middle layer

Figures 5 and 6 show the results of simulations for one TAN grade with two different stack layouts. In Figure 6 the maximum pressure at the front surface of the acceptor for different gap distances can be seen. The pressures are shown for all three layers separately. Also the boundaries of the critical initiation pressure that was determined from the GAP tests are shown. In Figure 6 it can be seen that the pressure at the acceptor is not a steadily decreasing function of the distance, some fluctuations can be seen, especially at small gap distances and for the upper layers. The fluctuations are caused by reflections of the blast wave from the donor. This wave is reflected by the floor/ground and also by the irregular surface shape of both donor and acceptor. The specific geometrical situation of the stack at a certain gap distance can therefore give rise to a

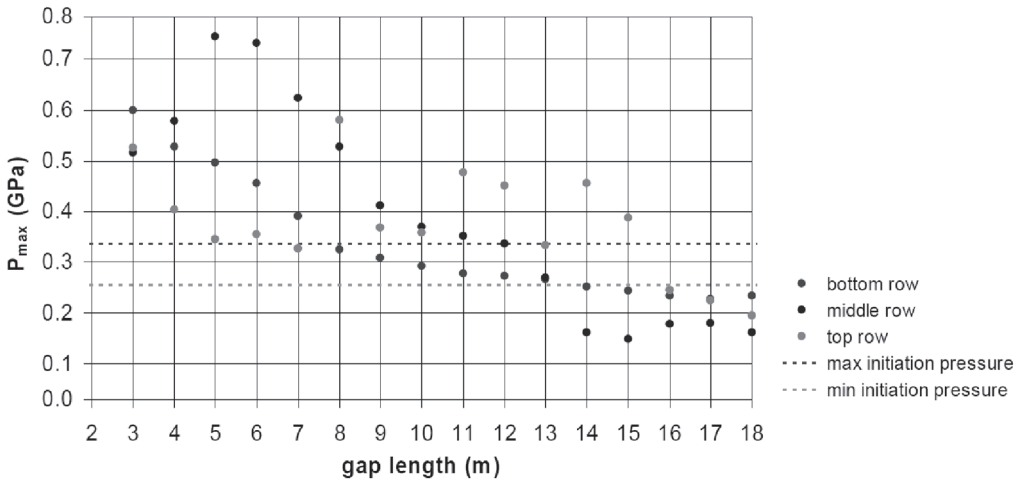

Figure 6. Results of the simulation with one grade of TAN and initiation point 3 (point initiation at top of middle layer).

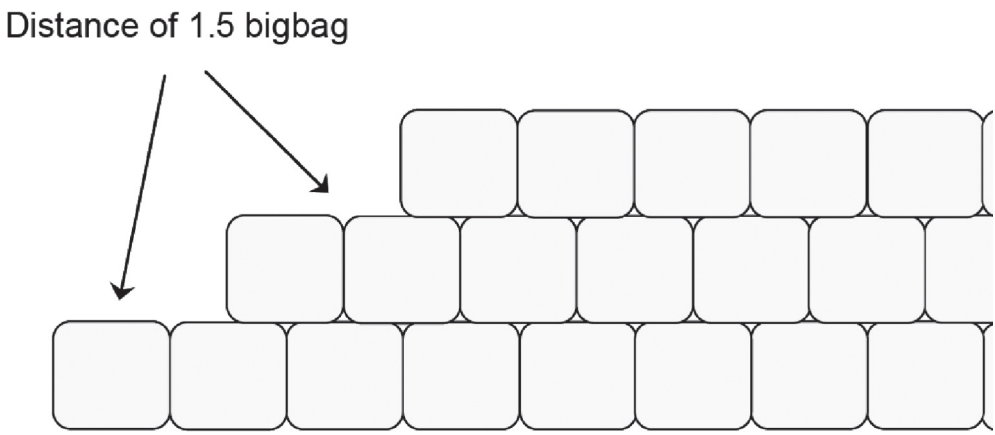

Figure 7: Revised stack layout.

higher pressure at specific levels of the acceptor than for the case with a shorter distance. For larger gap distances the pressure at the acceptor decreases more steadily with increasing gap length.

From simulations where different initiation points were used, it can be concluded that maximum pressure at the top layer of the acceptor is the highest in the gap range considered. For larger gaps the lower layer shows slightly higher pressures. The pressure levels at the lower layer are mainly the result of regular overall blast from the donor and have a long duration. The comparable pressure levels at the upper layers are slightly lower (due to the larger gap) but in addition the upper layers are more prone to be hit by turbulent reflection waves from the ground. These reflections results in pressure pulses of relatively larger magnitudes, but of short duration. It is not clear whether the duration of these pressure pulses are long enough to initiate the top layer.

These simulations gave a stack separation of 16 m (all points below min. initiation pressure line).

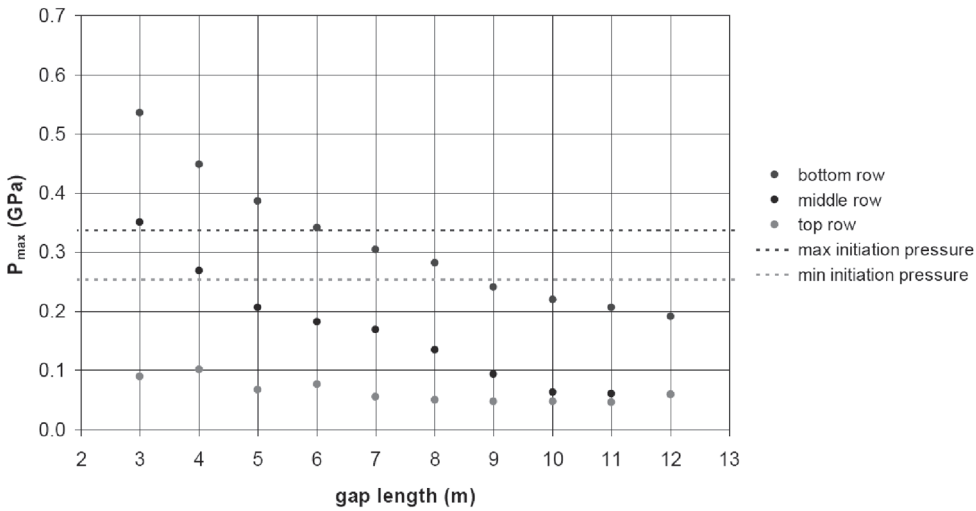

Figure 8: Results of the simulation with one grade of TAN (same as in Figure 7, but with revised stack layout) and initiation point 3 (point initiation at top of middle layer).

For the other samples tested, the stack separation distances varied between 9 m and 16 m.

Simulation showed that by changing the layout of the acceptor stack, the stack separation distances could be reduced:

In Figure 8 results of simulations with revised stack layout as shown in Figure 7 are shown. As can be seen the critical separation distance in this configuration (Figure 7 and 8) was reduced to 9 m. The critical separation distance was much smaller than for the 12+11+10 configuration, 9 m compared to 16 m for the 12+11+10 configuration. As shown in Figure 8 the pressure for all three layers is decreasing as a function of the distance, and no fluctuations due to reflecting pressure from the ground can be found. Because of the absence of reflecting pressure waves, the critical separation distance is much lower in the 12+9+6 configuration.

3. CONCLUSIONS

In this study the storage layout for porous ammonium nitrate (TAN) has been determined for three different grades. A number of gap tests have been performed to determine the critical separation distances between the test material and ANFO (as donor). Tube tests have also been performed to determine the blast effect of TAN on the surroundings. The results of these tests were used in simulations to determine critical initiation pressure, critical separation distances for given practical situations and the TNT equivalence of the materials.

From the tube tests the following conclusions can be drawn:

- All three test materials detonated in the tube test and the critical diameter of the materials is smaller than 1.16 m
- The TNT equivalence is dependent on the distance. Note that in the interpretation of the equivalence value it must be kept in mind that these tests were fully optimised to produce a maximum effect with respect to configuration, and a very strong initiation source was used
- In addition to the non-ideal effect in practical situations, the blast effects in the tests concluded that ammonium nitrate (TAN) does not possess the same effect behaviour as TNT. At short distances TAN gives a higher over-pressure effect, while the effect is smaller at larger distances. The TNT equivalences in the present work were determined at relatively short distances
- The TNT equivalence, used for practical

situations, is a combination of 'explosive power' and 'efficiency' (i.e., the part of the bulk which contributes to the blast effect in a detonation). The 'explosive power' is based on the TNT equivalence obtained in the tests. From a combination of the results of these tests, results of previously performed tests and the TNT equivalence determined in AN accidents, a TNT equivalence of about 20 % appears appropriate for practical situations. The value depends on the configuration of the stack, density and type of the material and the way of initiation

- With this value for the TNT equivalence the maximum allowable amount of TAN in one pile or stack can be determined, based on the maximum allowable overpressures in the surroundings (e.g. storage tanks, road)

From the results of the gap tests the critical initiation pressures were determined for the TAN grades tested.

Simulations were performed to determine the critical separation distances between stacks of big bags to prevent sympathetic detonations between the stacks. Contrary to dense, fertiliser grade AN, the critical separation distance for TAN depends on configuration of stacks, way of initiation and density and type of material. By altering stack shape the critical separation distance was reduced from 16 m to 9 m for one of the TAN samples tested. The other grades tested also showed similar reduction in stack separation distance.

It is very important to note that our tests were performed with TAN of high quality that had been stored properly. Any AN that is subjected to thermal cycling or absorption of water might dramatically change its properties and thereby become more sensitive.

4. ACKNOWLEDGEMENTS

We would like to thank TNO in The Netherlands and FOI in Sweden for conducting the tests and simulations.

REFERENCES

Baker, W. E. et al. 1983. Explosion hazards and evaluation. In: *Vol. 5 of Fundamental studies in engineering. Elsevier Science Publishers, Amsterdam, The Netherlands. ISBN 0-444-42094-0.*

Bauer, A., King, A. & Heater, R. 1979. The deflagration to detonation transition characteristics of molten ammonium nitrate. *The Canadian Fertilizer Institute and Contributing Bodies, The Department of Mining Engineering, Queen's University, Kingston, Ontario.*

Bauer, A., King, A. & and Heater, R. 1982, The explosion hazards of Ammonium Nitrate and Ammonium Nitrate based fertilizer compositions. *The Canadian Fertilizer Institute and Contributing Bodies, The Department of Mining Engineering, Queen's University, Kingston, Ontario.*

Kersten, R.J.A., van den Hengel, E.I.V. & van der Steen, A.C. 2006. Detonation Characteristics of Ammonium Nitrate Products. *IFA Technical Symposium, Vilnius, Lithuania.*

Kołaczkowski, A., Pękalski, A. & Meissner, Z. 2000. Estimation of the liability to detonating of prilled ammonium nitrate fertiliser grade. *Journ. of Loss Prevention in the Process Industries, Vol.13, Elsevier. 555- 561.*

Medard, L.A. 1989. Accidental explosions, Volume 1: Physical and Chemical Properties. *Published by Ellis Horwood limited, ISBN 0-7458-0403-9.*

Mouilleau, Y. & Dechy, N. 2002. Initial analysis of the damage observed in Toulouse after the accident that occurred on 21st September on the AZF site of the Grande Paroisse Company. *International ESMG Symposium, Nürnberg. Germany.*

NFPA 1968. Table of separation distances of ammonium nitrate and blasting agents from explosives or blasting agents. *Official Standard no.492, National Fire Protection Association, Quincy, Massachusetts.*

Van Dolah, R.W., Gibson, F.C. & Murphy, J.N. 1965. Sympathetic detonation of ammonium nitrate and ammonium nitrate fuel oil. *Explosives Research Centre, Bureau of Mines, Pittsburgh, Pa.*

Van den Hengel, E.I.V. 2007. Separation distances and TNT equivalence of three different types of TAN. TNO *Defence, Security and Safety, The Netherlands (Company restricted report).*

Vienna Conference Proceedings 2007, P. Moser et al.

Numerical simulation of the detonation products behind two head-on colliding detonation waves using the Davis Equation of State

K. Yang
Institute of Applied Physics and Computational Mathematics, Beijing 100088, China

X.M. Hu
National Key Laboratory of Computational Physics, Institute of Applied Physics and Computational Mathematics, Beijing 100088, China

Z.H. Wu
Institute of Applied Physics and Computational Mathematics, Beijing 100088, China

H. Pan
Institute of Applied Physics and Computational Mathematics, Beijing 100088, China

ABSTRACT: Employing the Davis equation of state, the expansion of metallic tubes induced by two head-on colliding detonation waves inside has been studied. The parameters of Davis EOS of JOB9003 are calibrated in the 2-D hydrokinetics program. Used the program to simulate the experiment of the expansion of metallic tubes induced by two head-on colliding detonation waves inside, the results are according with the experimental results. We also compared the results with the results calculated by JWL EOS. It indicates that Davis EOS can describe this experiment more accurately than JWL EOS.

1. INTRODUCTION

Following the development of design, simulation and formulation of high explosive, the research of equation of states of detonation products improves from experience to theory. It becomes important facility in the engineering field. The EOS with constant exponent form e.g. $P=A\rho^k$ is simple and easy to be used to simulate the detonation product. As we know, k is about 3 in the CJ point, but when the detonation product expands to low density just like ideal gas, k decrease to 1.3. The EOS with constant exponent form has some distance with true state. In order to calculate accurately the detonation capability, Jones, Wilkins and Lee et al. (1973) developed the JWL equation of state. Its application range is from 0.1GPa to CJ pressure. For the numerical simulation of detonation products that detonation pressure over CJ pressure, Davis analysed the physical property of detonation products and developed the Davis equation of state (Davis 1993). In this paper we used Davis EOS to calculate the expansion of metallic tubes induced by two head-on colliding detonation waves inside, and compare the calculation results with experiment.

2. DAVIS EQUATION OF STATE

Davis used the equation of state for detonation products to describe the state that detonation pressure over CJ pressure. Davis EOS with the

form p=p(ν,e) allows independent calibration of the adiabatic gamma and the Grüneisen gamma. The EOS is given by

$$p(v,e)=\frac{e}{v}[k-1+F(v)(1+b(1-\frac{e}{e^s(v)}))] \quad (1)$$

where F(ν) drops from a finite value at small ν to zero at large ν, k and b is constant, and $e^s(\nu)$ is the specific internal energy on the principal isentrope. If $e=e^s(\nu)$, Eq.(1) is the isentrope equation. F(ν) has the simple form:

$$F(v)=\frac{2a(v/v_c)^{-n}}{(v/v_c)^n+(v/v_c)^{-n}} \quad (2)$$

where a, n and ν_c is constant. From Eq.(2), the isentrope equation in the e-ν and p-ν plane is that:

$$e^s(v)=\frac{p_c v_c}{k-1+a}(\frac{v}{v_c})^{-(k-1+a)}[\frac{1}{2}(\frac{v}{v_c})^n+\frac{1}{2}(\frac{v}{v_c})^{-n}]^{a/n} \quad (3)$$

and

$$p^s(v)=p_c\frac{k-1+F(v)}{k-1+a}(\frac{v}{v_c})^{-(k+a)}[\frac{1}{2}(\frac{v}{v_c})^n+\frac{1}{2}(\frac{v}{v_c})^{-n}]^{a/n} \quad (4)$$

In above equation of state, there are six constants. That is k, a, n, ν_c, p_c and b. In order to get the four parameters a, n, ν_c and p_c, the follow four equations are simultaneously solved with k=1.3.

$$\gamma_J=k+F_J+\frac{4an}{(k-1+F_J)G_J^2} \quad (5)$$

$$p_J=p_c\frac{k-1+F_J}{k-1+a}(\frac{v_c}{v_J})^{k+a}(\frac{G_J}{2})^{a/n} \quad (6)$$

$$E_0=\frac{p_J(v_J/v_0)}{k-1+F_J}-\frac{1}{2}p_J(1-v_J/v_0) \quad (7)$$

$$E_0-1.115E_g=\frac{p_7(v_7/v_0)}{k-1+F_7} \quad (8)$$

where $G_J=(\nu_J/\nu_c)^n+(\nu_J/\nu_c)^{-n}$, $\nu_0=\rho_0^{-1}$ is explosive initial ratio volume and $\nu_7=7\nu_0$, p_J, ν_J, γ_J is respectively CJ detonation pressure, ratio volume and isentrope exponent. $E_0=\rho_0 e_0$ is explosive chemical energy per volume. Davis described this Equation of state in detail (Davis 1993).

3. CALCULATION MODEL AND DISCUSSION

We used 2-D hydrokinetics program to simulate the experiment (Chen 2003) of the expansion of metallic tubes induced by two head-on colliding detonation waves inside. We simulated the shot 5 and shot 6 that were mentioned in the reference (Chen 2003).

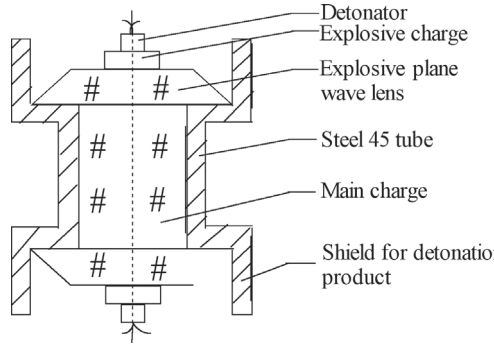

Fig.1 Experimental setup.

The experimental setup was shown in Fig.1. The main explosive is JOB-9003 with size Φ25.4mm×75mm. The thickness of the shot 5 and shot 6 is 3mm and 4mm respectively. The parameter used in the calculation is same with reference (Chen 2003). It was shown in Table 1. Parameterρ_0, c_0, S, v, Γ and Y is initial density, sound speed, shock Hugoniot parameter, Poisson ratio, Gruneisen parameter and yield strength respectively. The Davis EOS has been used to describe the behavior of the detonation products of explosive JOB-9003. The density of explosive JOB-9003 is ρ_0 = 1.844g/cm^3, and the detonation velocity is 8.74 km/s(Sun,2000).

Table 1. Data for metallic tube material

material	ρ_0 (g/cm^3)	c_0 (km/s)	S	v	Γ	Y(GPa)
steel 45	7.92	4.580	1.510	0.290	2.02	0.75

Fig. 2(a) shows the metallic tube surface displacement history of shot 5 (the thickness of tube is 3mm). The distance between measure point and initiation point is 21.7mm. Fig. 2(b) shows the displacement history of head-on. The displacement history of head-on and single detonation (22.0mm away from the initiation point) of shot 6 was shown in Fig.3. We fitted the expansion velocity calculational results of the metallic tube surface. The results of calculation and experiment were shown in Table 2.

It is apparent from Fig. 2, Fig. 3 and Table 2 that the calculation results accord with the experimental results by using Davis EOS to describe the

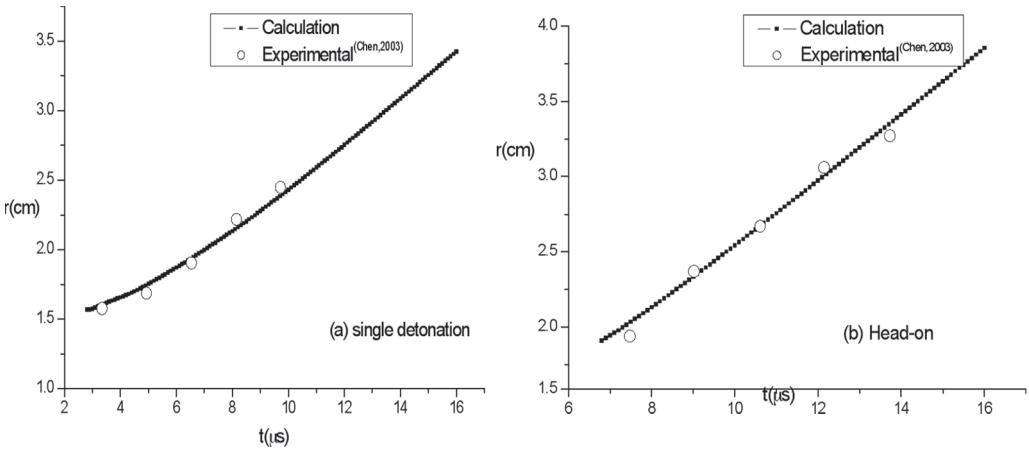

Fig.2 Calculation of the displacement history of shot 5.

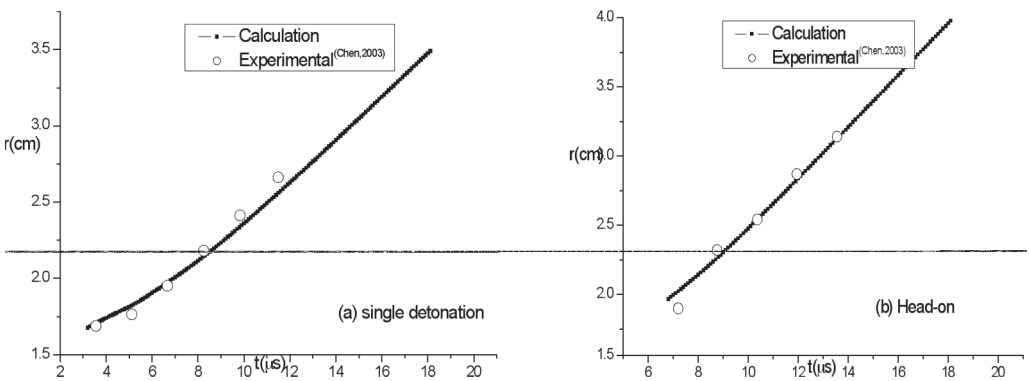

Fig.3 Calculation of the displacement history of shot 6.

Table 2. Comparison of experimental and calculation.

expansion velocity(cm/μs)	Shot 5 Single detonation	Shot 5 Head-on	Shot 6 Single detonation	Shot 6 Head-on
experimental	0.14±0.01	0.22±0.01	0.13±0.01	0.19±0.01
calculation	0.145	0.214	0.125	0.181

detonation products, especially for head-on. The calculation results indicated that the metallic tube surface expansion velocity of the head-on is 1.48 times than the single detonations for shot 5. For shot 6, the value is 1.45. The Davis EOS can describe the problem of overdriven detonation more accurately. When the state of detonation products lies above CJ point in the p-v plane, the Davis EOS can describe the work capacity of detonation products more accurately.

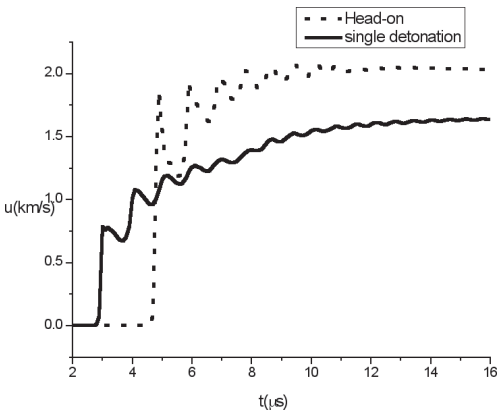

Fig.4 Surface velocities of the tube of shot 5.

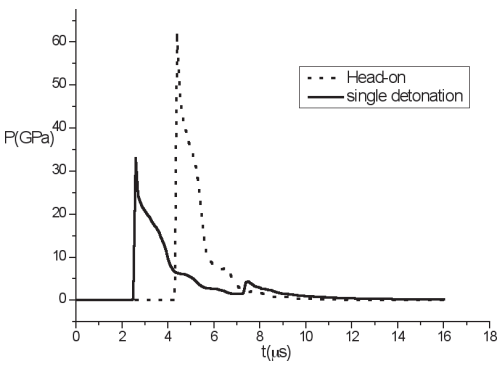

Fig.5 Pressure curves of detonation product of shot 5.

Fig. 4 shows the calculation results of the metallic tube's surface velocities. The expansion velocity of head-on is different from that of single detonation. The expansion velocity's peak value of head-on is obviously bigger than the latter. As the shock wave arrived first, the surface velocity of single detonation reached up to 0.78 km/s in a short time, and the peak velocity of head-on is 1.86 km/s. Then the velocity evolved gradually to a fixed value. For single detonation, the value is 1.64 km/s; for head-on, that is 2.04 km/s. Fig. 5 shows that the peak pressure of head-on reached up to 62.4 GPa, and that of single detonation is 33.0 GPa.

4. CONCLUSIONS

Employing the Davis equation of state, the problem of overdriven detonation has been described. We simulated the experiment of the expansion of metallic tubes induced by two head-on colliding detonation waves inside. The conclusion is that the calculated results are according with the experimental results. It indicates that Davis EOS can accurately describe the state of detonation products that detonation pressure over CJ pressure.

REFERENCES

Lee, E., Finger, M., Collins, W., 1973. JWL equation of state coefficients for high explosives. *Lawrence Livermore Laboratory Report*, UCID-16189.

Davis, W.C., 1993. Equation of state for detonation products. *Proceeding of the 10th symposium(Int.) on detonation*, 12 July 1993, Boston,MA.

Chen, J., Sun, C.W., Pu, Z.M., et al. 2003. Expansion of metallic tubes by detonation product behind two head-on colliding detonation waves. *Explosion and Shock Waves*, 2003,23(5): 442-447.

Sun, C.W., Wei, Y.Z., Zhou, Z.K., 2000. *Applied Detonation Physics*. Beijing: Defense Industry Press, 2000, (in Chinese).

Vienna Conference Proceedings 2007, P. Moser et al

Research on the influence of Guar-M-207 on the water resistance of industrial explosives

V. Mitkov
'Videx' JSC, Sofia, Bulgaria

ABSTRACT: Research and development work is being done in the Republic of Bulgaria to fulfill the government programme on utilization of surplus ammunition and reuse of propellants extracted from it (referred to as 'secondary propellants' later in the text) as sensitizers in water-based explosives for civil purposes. New water-based explosives with secondary propellants should have an excellent water resistance and necessary density. A study has been done for determination of the most appropriate quantity of the chosen Guar-M-207 thickener in the composition of the new water-based explosive mixtures. The influence of the amount of thickener on the water resistance (solubility) of water-based explosives was examined. The research carried out showed that stable results are obtained in case of the content of thickener in the mixture varying from 0.5 to 1.0% at which after 24 hours the solubility of the components is 10-12% which is totally satisfactory. Besides, the dependence of the quantity of thickener and the density of the explosive was determined.

1. INTRODUCTION

Research and development work has been carried out in the Republic of Bulgaria to fulfill the government programme on utilization of considerable quantities of surplus ammunition. One of the purposes was to find a safe, effective and ecological way to utilize all secondary products and elements of useless ammunition. As it is well known, unloading techniques have a specific character which must be observed when dealing with ammunition.

Ammunition is known to contain substances sensitive to mechanical and thermal impact. That is why there is a potential danger when they are processed. A casual detonation of one shell in a place where considerable quantities of ammunition are stored can, in many cases, cause tragic results. Furthermore, ammunition is generally not intended for disassembling and extraction of explosives. Having said that, one can infer that the process of disassembling and extraction of explosives is reasonably straightforward, however it encompasses some danger.

Bearing all this in mind, the development of methods, technology and equipment with the necessary instruments for carrying out safe and effective dismantling of shots and extraction of secondary propellants is an important and significant part of work on execution of the government program.

A principle scheme of the sequence and kinds of activities and operations on dismantling ammunition has been developed on the basis of the analysis conducted and the study of the main characteristics and structures of different types of ammunition subject to utilization. The purpose is to accomplish

total dismantling of needless ammunition through complete separation and extraction of fragmentation and missile explosives (Kambourova and Mitkov 2007).

Special attention was paid to the propellants contained in useless ammunition, their study, examination of their properties and estimation of possibility for their recycling as sensitizers in water-based explosives of Slurry type through total change of TNT sensitizers.

2. MAJOR CHARACTERISTICS OF WASTE PROPELLANTS EXTRACTED FROM USELESS AMMUNITION

The analysis carried out of powders extracted from missile charges of surplus ammunition showed that they can be divided in the following main groups: pyroxylin, nitroglycerine and diglycol. 51% of the propellants extracted from surplus ammunition are pyroxylin propellants and about 41% are nitroglycerine and diglycol propellants which are of major importance for production of civil explosives.

2.1 General appearance of secondary propellants

Figure 1 shows the general appearance of secondary seven-channel pyroxylin propellant of 9/7 brand. Powder grains have a cylinder form with a diameter of 5.86 mm, length - 12.6 mm and web thickness - 1.2 mm.

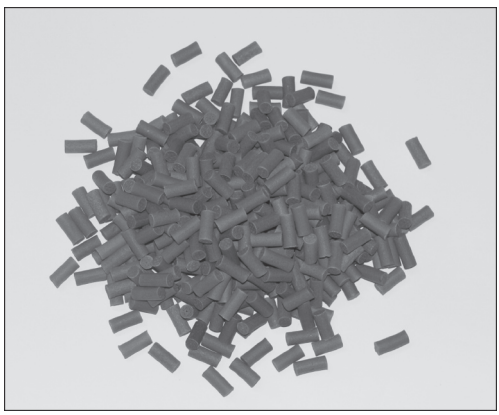

Figure 1. General appearance of seven-channel pyroxylin propellant with volatile dissolvent of 9/7 brand.

Figure 2 displays the general appearance of secondary one-channel pyroxylin propellant with volatile dissolvent of 4/1 brand. Powder grains have a form of a thin cylinder with a diameter of 1.4 mm, length - 8.0 mm and web thickness – 0.6 mm.

Figure 2. General appearance of one-channel pyroxylin propellant with volatile dissolvent of 4/1 brand obtained from useless ammunition.

Figure 3 presents the general appearance of secondary one-channel pyroxylin propellant with volatile dissolvent of 18/1 brand. The powder looks like cylinder sticks with a diameter of 5.5 mm, length - 380 mm and web thickness -1.95 mm.

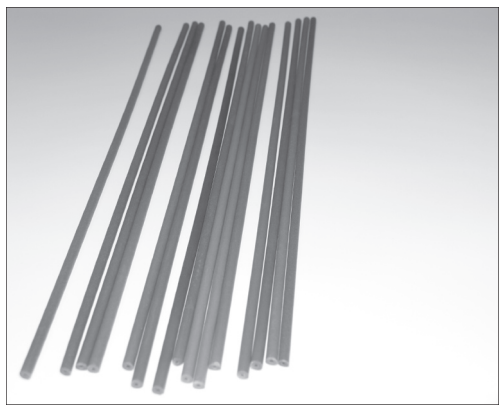

Figure 3. General appearance of one-channel pyroxylin propellant with volatile dissolvent of 18/1 brand obtained from useless ammunition.

Figures 4 and 5 show the general appearance of nitroglycerine one-channel propellant with almost non volatile dissolvent with added dinitrotoluene of NDT-3 18/1 brand. The powder presents cylinder

sticks with a diameter of 6.1 mm, length - 260 mm and web thickness – 1.77 mm.

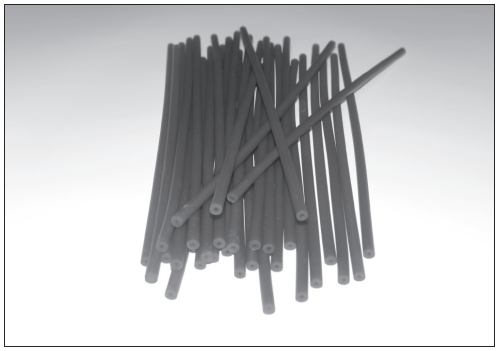

Figure 4. General appearance of one-channel pyroxylin propellant with almost non volatile dissolvent with added dinitrotoulene of NDT-3 18/1 brand obtained from useless ammunition.

Figure 5. General appearance of nitroglycerine powder of NDT-3 18/1 brand additionally ground to be placed in water-based explosives.

2.2 Quality characteristics of secondary propellants

Research on thermal and chemical resistance, sensitivity to impact, water resistance, primary initializing impulse and other parameters of the material obtained from dismantling pyroxylin and nitroglycerine propellants has been carried out (Kambourova and Mitkov 2005-2007).

Propellants of 18/1 and NDT-3 18/1 brands presenting long cylinders are ground through grinding in a specially designed mill in order to be used as sensitizers in explosives of Slurry type. The other brands of extracted propellant given in figure 1 and 2 can be used in explosives for civil purposes without being additionally processed.

The qualitative and quantitative study of secondary propellants showed the following:

- Nitroglycerine and pyroxylin propellants obtained from surplus ammunition were produced 25-30 and more years ago. General examination of the propellants after their extraction shows that they are perfectly preserved, structured and have shiny grains
- Tests of thermal resistance of secondary propellants after 48 hours in a chamber at 75±20°C show that they don't endure any physical or chemical changes as their grains stay shiny, loose, practically without any loss of weight that means lack of reaction
- Tests of chemical stability of pyroxylin propellants in a chamber at 95±0.50°C indicate that after 17 days at these conditions they practically don't lose weight or release brown fumes
- The tested brands of secondary propellants have an excellent water resistance and after 96 hours in water remain practically the same
- Sensitivity to impact of different brands of secondary propellants according to EN 13631-4 is over 5.0J, that is they are not affected by an impact of 5.0J

The research conducted shows that propellants extracted from useless ammunition have completely preserved properties and can be used as sensitizers in different brands of explosives for civil purposes after developing the necessary equipment and technology.

3. STUDYING AND CHOOSING THE MOST SUITABLE THICKENERS FOR EXPLOSIVES OF SLURRY TYPE

3.1 Thickeners used up to now

Determination and study of the most suitable thickener, as well as its optimum content in the blasting mixture, is of great importance when creating explosives with secondary propellants as sensitizers.

Until the present time the most common thickeners used in the Republic of Bulgaria, Russia and a number of east European countries have been carboximethylcellulose (KMC) and acrylamide. In Bulgaria, from 2 to 4% of the

thickener KCM have been used up to now in existing explosives of Slurry type which can't provide the necessary water resistance. After 24 hours in water these explosives lose from 30 to 40 % of their components which is extremely unsatisfactory (EN 13631-2).

In the process of developing new explosives for civil purposes with TNT sensitizer, a considerably more effective thickener of the Guar gum series, Guar-M-207, was chosen for work (EN 13631-4, EN 13631-5). Using the thickener Guar-M-207 made it possible to obtain an excellent water resistance of the water-based explosive of Slurry type 'Videxit' as after 24 hours the water resistance is equal to 9-10% and the content of thickener varying from 0.5 to 1.0%.

The excellent water resistance obtained when using the thickener mentioned above was confirmed by the blasting tests conducted in flooded ground with water flowing into 90 mm diameter drill holes. Using the explosive 'Videxit' in such hard conditions ensured excellent results while blasting at the hydro-electric plant 'Tsankov kamak'.

3.2 Determination of the most suitable quantity of the thickener in Slurry explosives

To determine the most suitable quantity of thickener for water-based explosives for civil purposes, with recycled propellants extracted from useless ammunition, the thickener Guar-M-207 in the explosive 'Videxit' was used.

3.2.1 Research methods

In the EC, EN 13631-5 standard for determination of water resistance of explosives in order to execute the directive 93/15 EEC concerning harmonization of the requirements related to trade and use of explosives for civil purposes was developed and admitted. According to this standard, after checking the solidness of the package if there is any, a charge is made from the test explosive with the total length of 0.5 m.

The test charge is placed in a vessel under a 200 mm water column for 5 hours, after that it is initiated and the detonation velocity is measured.

The operative EC standard for determination of water resistance of explosives for civil

Table 1. Solubility in water (water resistance) of water-based explosives with secondary propellants as a sensitizer depending on the content of the thickener Guar-M-207.

№	Amount of thickener,%	Density of sample,kg/m^3	Solubility in water, %				
			6h	12h	24h	48h	72h
1	Content 0.5	1430	6.15	9.27	12.85	15.08	15.33
2	Content 0.5	1425	6.20	9.19	12.80	15.03	15.27
3	Content 0.5	1420	6.159	9.23	12.73	15.02	15.27
	Average 0.5	1425	6.18	9.22	12.79	15.04	15.29
1	Content 1.0	1410	4.50	8.75	10.04	14.84	15.08
2	Content 1.0	1415	4.60	8.80	10.01	14.78	15.15
3	Content 1.0	1405	4.40	8.85	10.02	14.79	15.06
	Average 1.0	1410	4.50	8.80	10.02	14.80	15.10
1	Content 2.0	1400	4.30	8.45	9.98	14.27	14.82
2	Content 2.0	1405	4.26	8.35	9.79	14.23	14.60
3	Content 2.0	1395	4.20	8.40	9.92	14.15	14.68
	Average 2.0	1400	4.25	8.40	9.90	14.22	14.70
1	Content 3.0	1385	4.15	7.95	9.68	13.95	14.25
1	Content 3.0	1375	4.05	8.05	9.55	13.99	14.15
1	Content 3.0	1380	4.10	8.00	9.57	14.05	14.20
	Average 3.0	1380	4.10	8.00	9.60	14.00	14.20

purposes answers the question if the explosive preserves its blasting characteristics and properties after a certain period of time in water. This parameter is of special importance in practice but can't explain how the quantity of the chosen thickener affects the water resistance of the explosive.

A new method has been developed for the present research related to determination of the influence of the thickener Guar-M-207 content on water the resistance of the components for a longer period of time. According to this method, the test sample is put in water without a coat and after that the solubility of components of the explosive is measured. In fact, the sample is wrapped in cheese-cloth and sunk in a graduated cylinder filled with water. The solubility of the components in relation to the total mass of the test samples is observed in intervals of 6, 12, 24 and more hours. Thus the most suitable quantity of the thickener Guar-M-207 can be determined on the basis of the data obtained from the tests.

3.2.2 Results

According to the method described in 3.2.1 a series of 3 tests were carried out to determine the solubility of components of the new water-based explosives with secondary propellants as a sensitizer, with the content of the thickener Guar-M-207 ranging from 0.5 to 3 %. Table 1 shows the obtained results. The test samples weighed 200g.

Figure 6 shows the correlation between the solubility of components of the explosives with recycled propellant as a sensitizer and the content of the thickener after 6 and 24 hour stay of the samples in water.

Figure 7 displays the correlation between the solubility of components and the content of the thickener Guar-M-207 depending on the length of stay in water of the explosives with recycled propellant as a sensitizer.

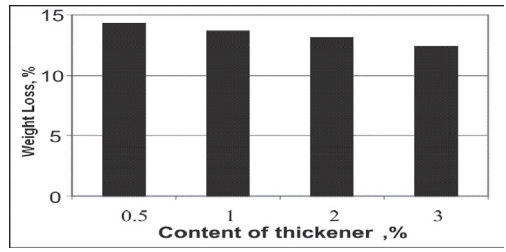

Figure 6a.

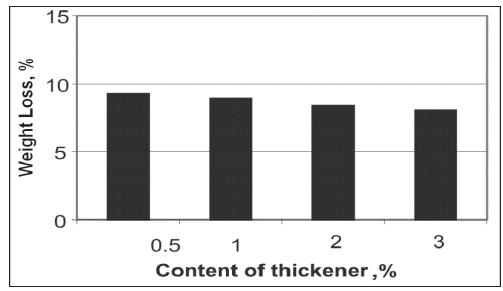

Figure 6b.

Figure 6. Solubility of explosives with recycled propellant as a sensitizer a) after 6 hours in water, b) after 24 hours in water.

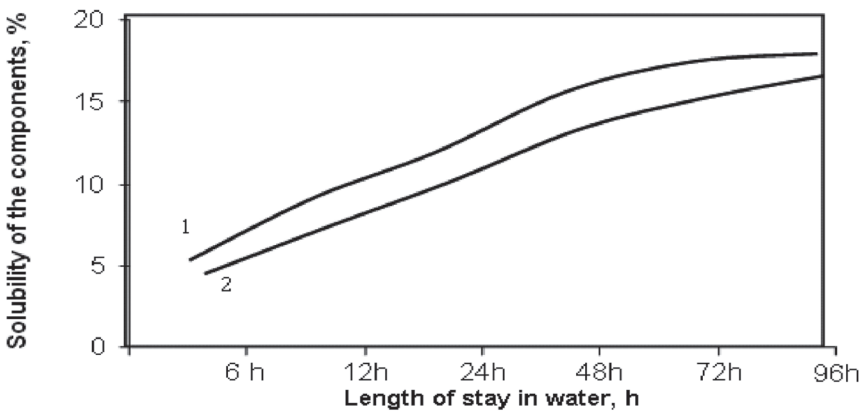

Figure 7. Solubility of the components depending on the content of the thickener Guar-M-207 and stay in water , 1- for the content 0.5%, 2- for the content 1%.

4. CONCLUSIONS

The analysis of the results obtained from the research of the influence of Guar-M-207 thickener on the water resistance of explosives with secondary propellant as a sensitizer makes it possible to draw the following main conclusions:

- Pyroxylin and nitroglycerine propellants with completely preserved physical and chemical characteristics and properties can be extracted from useless ammunition
- Recycled propellants can be successfully used as sensitizers in water-based explosives for civil purposes
- Work with the thickener Guar-M-207 ensures excellent water resistance of the new explosives and completely satisfactory density of over 1350 kg/m^3
- Water resistance of blasting mixtures at the content of the thickener varying from 0.5 to 3% doesn't differ significantly and equals to 4 - 6% solubility after 6 hours and 8 - 9% after 12 hours which is totally satisfactory
- Further development of the project stipulates the amount of the chosen thickener to be 0.5% which provides excellent blasting parameters of the water-based explosives with a sensitizer of propellants extracted from useless ammunition

REFERENCES

Kambourova, G. & Mitkov, V. 2007. Research on thermal and chemical stability of propellants extracted from useless ammunition, *Jour. Explosive', issue 5*. Sofia: 17-21.

Kambourova, G. & Mitkov, V. 2006. Research on sensitivity to impact of propellants obtained from useless ammunition according to the new requirements of the EC, *Annual of MGU, vol. 49*. Sofia: 123-127.

Kambourova, G. & Mitkov, V. 2007. Research on water resistance of propellants extracted from useless ammunition, *Jour. 'Explosive', issue 5*. Sofia: 25-28.

Kambourova, G. et al. 2005. Research on seismic effect on the guarded objects while conducting blasting activities at the hydro and electric plant 'Tzankov kamuk', subordinate object 'Deflection canal', *Jour. 'Explosive', issue 3*. Sofia: 19-26.

Lazarov, S. 1998. Blasting activities, Sofia: Tehnika.

Mitkov, V. & Kambourova, G. 2005. Study and development of new water-based and water resistant explosives of Slurry type, Jour. *'Explosive', issue 2*. Sofia: 23-26.

Mitkov, V. 2006. Determination of the most suitable quantity of the thickener Guar-M-207 as well as the water resistance and density of the new blasting mixtures, *Jour. 'Explosive', issue 4*. Sofia: 15-16.

Mitkov, V. & Kambourova, G. 2006. Method, technology and equipment for dismantling useless ammunition and extraction of propellants from it, *Annual of MGU, vol. 49*. Sofia: 135-139.

Mitkov, V. & Kambourova, G. 2006. Research and development of water-gel explosives of Slurry type for civil purposes with a sensitizer obtained from useless ammunition, *International Conference on Blasting Techniques. Slovak* Republic: Slara Lesna, 32-42.

CEN 2002. Explosives for civil uses – High explosives – Part 2: Determination of thermal stability of explosives. *EN 13631-2*. Brussels: European Committee for Standardization.

CEN 2002. Explosives for civil uses – High explosives – Part 4: Determination of sensitiveness to impact of explosives. *EN 13631-4*. Brussels: European Committee for Standardization.

CEN 2002. Explosives for civil uses – High explosives – Part 5: Determination of resistance to water. *EN 13631-5*. Brussels: European Committee for Standardization.

Vienna Conference Proceedings 2007, P. Moser et al.

Safe blasting near the historical caves of Tourah, Cairo, Egypt

M. Khaled
ASEC Company for Mining ASCOM, Egypt

K. Abdel Rahman
National Researches Inst. of Astronomy & Geophysics, Cairo, Egypt

E. Bagy
ASEC Company for Mining ASCOM, Egypt

ABSTRACT: A number of blasts using specific blasting techniques were performed at the limestone quarry of Tourah Portland Cement Company (TPCC), to assess the blast vibrations. Initially, the amplitude of vibration velocity was measured at both Near-Field and Far-Field, and the attenuation rate of peak particle velocity (PPV) in relation to distance was calculated. Later the study was extended to include the effect of azimuth at different profiles, and the data was analyzed and contoured onto a map covering the quarry area. Using the contour map, the effect of azimuth and its attenuation rate at different directions could be predicted.

This study helped TPCC limestone quarry to remain open and also to extend, by convincing the authorities that the blasting operations there are safe, regarding the nearby caves. The authors found that the authorities restrictions are unreasonably low, needlessly increasing the cost of the blasting operations, and decreasing the quarry productivity.

1. INTRODUCTION

There are four large cement factories, located nearby Cairo metropolitan. Blasting operations are used to extract the limestone from the quarries for cement industries. All the quarries have to keep the blast vibrations under control. The oldest quarry of these is TPCC limestone quarry owned by Italcementi Group, which lies near to some historical caves, within Tourah Mountain as shown in Figure 1.

Some previous blasting produced high PPV values, upsetting the local authorities, which express concern about cave stability during the future blasting. In 2005 TPCC recognized the need for advanced drilling and blasting. They selected ASEC Company for Mining ASCOM as a company that specializes in quarry management throughout Egypt and the Middle East.

Three similar deck charges were designed in the blast hole of the lower bench with 55.0 m, while only two deck charges for the upper bench with 35.0 m height. In each deck, the maximum instantaneous charge weight is 20 kg of gelatin dynamite (primering), and 180 kg ANFO (blasting agent), to keep the total explosive charge per blast not more than 3 ton, to comply the local authorities

restrictions, as illustrated in Figure 2.

Figure 1. Tourah caves.

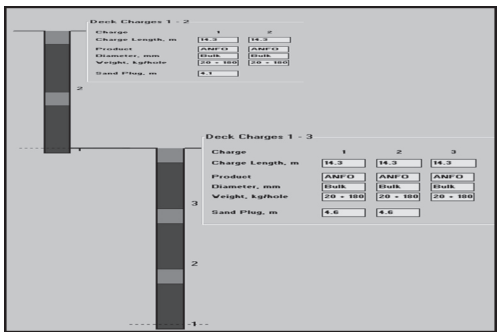

Figure 2. Charging plane.

2. LOACTION AND GEOLOGY

The limestone quarry of TPCC is opened at the southwestern foot slopes of Tourah Mountain, which forms the eastern high escarpments overlooking the Nile River, and situated 23 km south of Cairo, on Maadi - Helwan road, as in Figure (3), geologically this area belongs to Mokattam Formation (Middle Eocene).

The quarry deposit is mainly composed of thick bedded limestone, mostly earthy white to faint yellow in the upper 60.0 m, turning to grayish yellow and grey downwards. In the upper 60.0 m, two segments of 4.0 m each are composed of nodular limestone. The hardness of the limestone deposit varies from moderately hard to very hard. Fissures are more frequent in the upper bench and less downwards. Most of these fissures are filled with iron oxides and siliceous materials. The noticeable structures in the area are a group of step faults running east-west, and perpendicular to the investigated site.

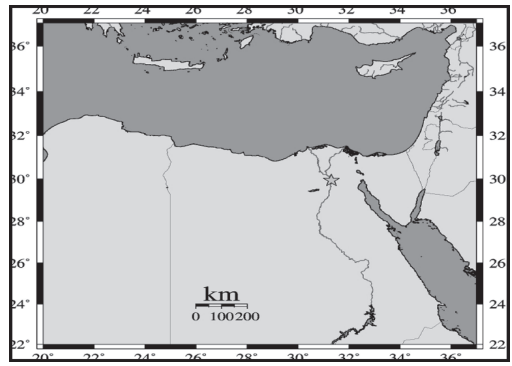

Figure 3. Location map of the investigated site.

3. QUARRY OPERATION

TPCC limestone quarry faces form a more or less semi-circular shape, with a circumference of 2.8 km. The quarry consists of two benches, the upper bench varying in thickness, depending on the surface topography with average 35.0 m. while the thickness of the lower bench attains approximately 55.0 m, as shown in Figure 4.

The limestone is excavated by drilling and blasting. The material blasted from the upper bench is pushed by bulldozers from bench down to the quarry floor, and all loading and hauling operations are performed at the quarry floor. In order to keep the upper bench suitable as a drilling and blasting bench, its width is constantly kept narrow, and ranging between 5 to 10 m.

Figure 4. TPPC limestone quarry benches.

4. INVESTIGATION PROGRAMME

The local authorities arranged many restrictions for the blasting operations in TPCC limestone quarry, in order to protect Tourah caves from blasting vibrations. One of these restrictions is lowering the maximum explosives charge to 3 ton per blast, and the maximum permitted (PPV) is 5.0 mm/second. In order to negotiate with the local authorities about their restrictions, a long term investigations program was established and preformed by ASCOM in 2006, in three steps, as following:

- The objectives of the first step (previous study) were to derive the optimum time intervals, and the effect of using certain appropriate initiation (top or bottom), which could then be employed to minimize PPV produced in both upper and lower benches. It is also highlighted the advantage of using non-electrical detonators, (for the first time in Egypt) in comparison with the conventional electrical detonators. Also the scaled distance at the maximum permitted PPV value was calculated. The results were previously published in 33rd ISEE Conference (Khaled et al. 2007).
- It was planned that the second step (present study) would be to calculate the attenuation rate of PPV in relation to distance, at both near-field and far-field. Then the study was extended to include the effect of azimuth at different profiles and contouring PPV values into maps covering the quarry area. Using these maps the azimuth effect and the attenuation rate of PPV on different directions, at Tourah caves could be predicted.
- While the investigation protocols pointed that the next logical step will be to study the advantages of using electronic detonators (for the first trial in Egypt) in minimizing PPV values.

5. ATTENTUATION EFFECT

Series of blasts were monitored with four digital strong motion instruments (REF TEK-130 SMA), deployed in a linear array, in order to estimate the attenuation rate of PPV (decreases in vibration amplitude with distance), in both of Near-Field and Far-Field, at distances of (30 – 100 m) and (500 – 900 m) respectively from the shot-point.

All blasts are similar, to great extent, in the burden (6.0 m), spacing (8.0 m), hole diameter (165.0 mm), and deck charge weight loadings (200 kg). The key variables were the different detonators timing intervals and the initiation system (electrical and non-electrical detonators), also some blasts were bottom initiated, while others were top initiated. Different blasting techniques were used, as the attenuation rate of PPV is related mainly to the effect of local geological conditions of the site, and not to the type of the used technique.

5.1 Near-field attenuation

Four blasts were preformed at the Near-Field of the shot-point. The value of attenuation rate of PPV in the upper bench was calculated from the best-fit equation in Figure 5, and it was - 1.15. In the case of the lower bench the attenuation rate of PPV was - 0.32, as in Figure 6. It is noticed from the above figures that, the attenuation rate in the upper bench is greater than in the lower bench. This is because the limestone in the upper bench is anisotropic and fissured, so its absorption of seismic energy is very high. While the low rate of attenuation of PPV in the lower bench can be attributed to the compacted characteristics of limestone in the lower bench. Moreover, the geometrical spreading minimizes the seismic energy density as the distance from the shot-point increases. This is matched well with the previous study.

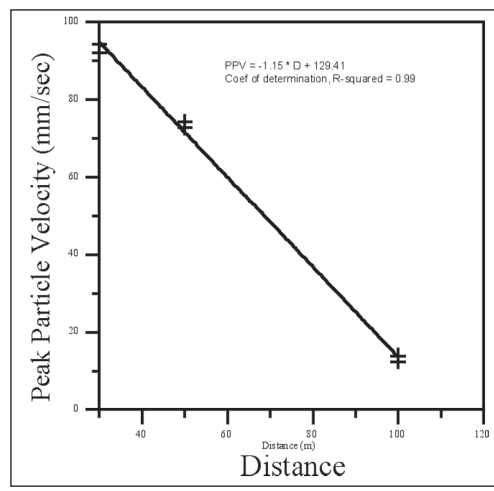

Figure 5. Near-field attenuation of PPV for the upper bench.

5.2 Far-field attenuation

The wave motion spreads concentrically from the blast site, particularly along the ground surface, and is therefore attenuated, since its fixed energy is spread over a greater and greater mass of material as it moves away from its origin. Even through it attenuates with distance the motion from a large blast can be perceived from faraway, (Dowding 1985).

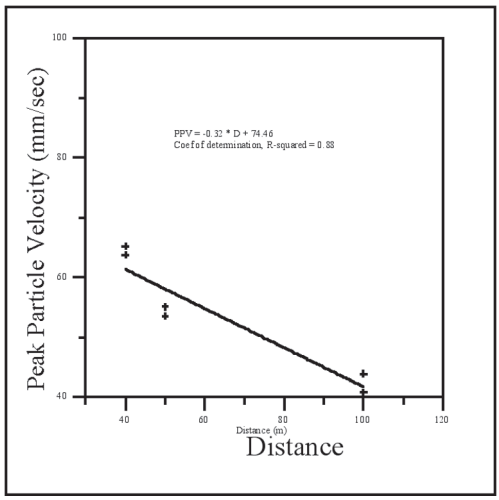

Figure 6. Near-field attenuation of PPV for the lower bench.

Ten blasts were preformed in the far-field of TPCC limestone quarry, and divided between the quarry benches (upper and lower). Figures 7 & 8 showed the following observations:

- The attenuation rate of PPV in the Far-Field was - 0.003 at the upper bench, and is not significantly different from that of the lower bench. This may be reflects the minor influences of the geological conditions of limestone between the upper and lower benches.
- The attenuation rate at distance about 700 m from the shot-point decreased abruptly, and this may be attributed to the presence of a topographically low area (wadi), at this distance.
- The values of attenuation rate of PPV were sharply decreased in the Near-Field, than the Far-Field, due to the effects of the geometrical spreading and the absorption factor of the seismic energy within the limestone deposit of upper bench.

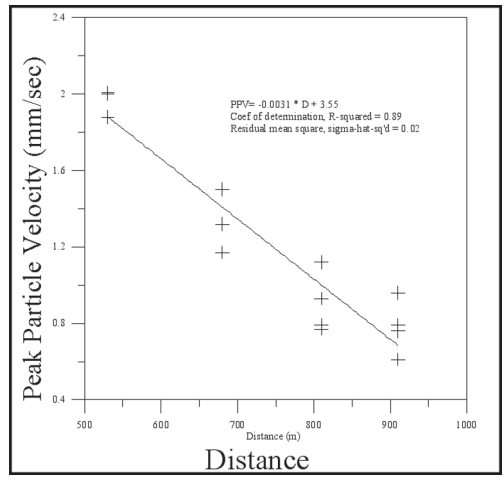

Figure 7. Far-field attenuation of PPV for the upper bench.

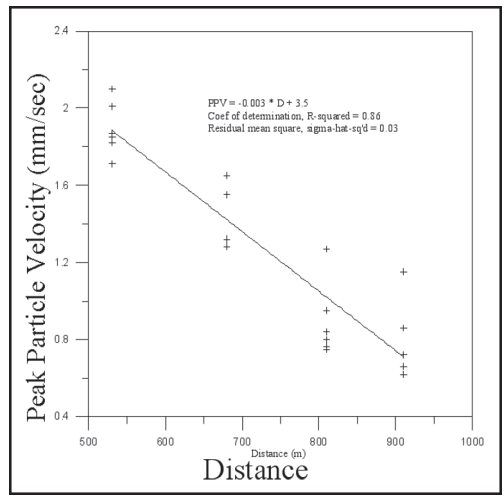

Figure 8. Far-field attenuation of PPV for the lower bench.

6. AZIMUTH EFFECT

Series of other blasts were recorded by three component velocity sensors (Instantel-Minimate Blaster), installed at a constant distances (100, 150 and 200 m) from the shot-point, along azimuthally different profiles radiated from the quarry face. A standard blast design was selected in order to define the direction of yielded optimum PPV values. All

blasts were initiated by non-electrical system, with an inter-deck timing 25 millisecond, and an inter-hole timing 42 millisecond.

It is evident from the distribution of data in Figures (9) and (10), that there is no clear relationship between the azimuth and the resulted PPV values in all directions. This means that, the radiated energy from each blast not equally transferred in all directions, and this reflects the heterogeneity of the deposit, especially in the upper bench.

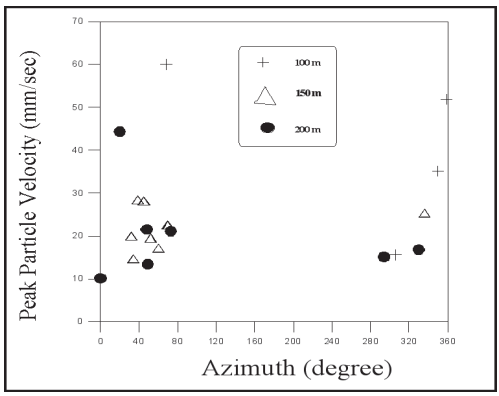

Figure 9. Relationship between azimuth and PPV for the upper Bench.

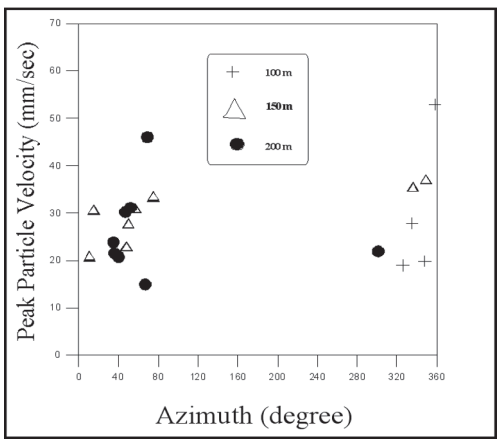

Figure 10. Relationship between azimuth and PPV for the lower Bench.

Aimone-Martin (2007) stated that, the variation in attenuation in the different directions is not statistically significant and does not warrant special regulatory consideration. This is well correlated with our observation.

This reflects the different factors that constitute the azimuth effects as following:

- Presence, frequency and directions of fissures and joints in the investigated site, as well as the type of fissure filling materials affected the values of PPV, and its rate of attenuation.
- Elevation of the measuring points; some times there is a direct relationship between the values PPV and the sensor elevation.
- Type and thickness of the over-burden materials; as the thickness of loose materials increased, the PPV values tended to be minimized.

7. SCALED DISTANCE

Scaled distance is defined as the dimensionless parameter for distance. It is derived as a combination of distance and charge weight influencing PPV value.

$$PPV = \frac{K}{\left(\frac{R}{\sqrt{W}}\right)}\alpha \qquad (1)$$

The above equation depended on two constant factors. Where (K) represents the initial energy transformed from explosives to the surrounding rocks, and it is the line intercept at Scaled Distance = 1 on log-log graph, and (α) represents the attenuation rate of PPV, and it is the slop of the fitting line. The (W) and (R) are the maximum explosive charge per delay, and the distance from shot point respectively.

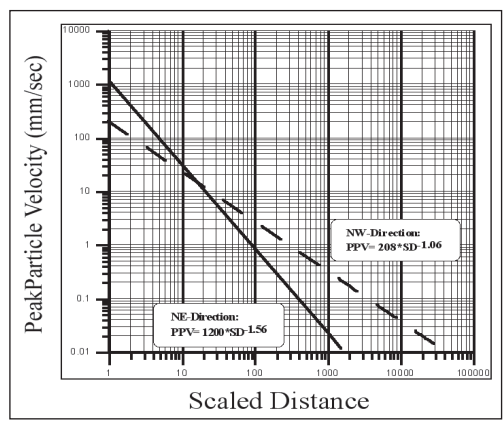

Figure 11. Scaled distance for NE & NW directions.

To assess the azimuth effect on the PPV values and its rate of attenuation, for the upper bench, the above mentioned constants have been determined for two curves represent both of NE and NW directions. This was found to be more precisely than one curve for the whole area.

From Figure 11 the following, equations were derived.

$$\text{NE – direction: } PPV = 1200\ (R / \sqrt{W})^{-1.56} \quad (2)$$

$$\text{NW – direction: } PPV = 208\ (R / \sqrt{W})^{-1.06} \quad (3)$$

The predicted values of PPV have been calculated at different distances along both profiles, Figure 12. It is evident that the NE direction yields significantly high PPV value, combined with high rate of attenuation. This means that, the PPV value was initially higher at NE than NW direction, and then abruptly decreased.

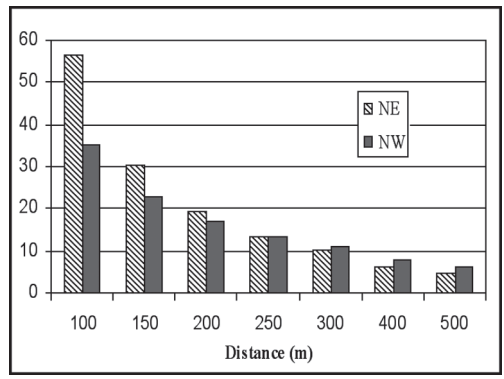

Figure 12. Predicted PPV values for NE & NW directions.

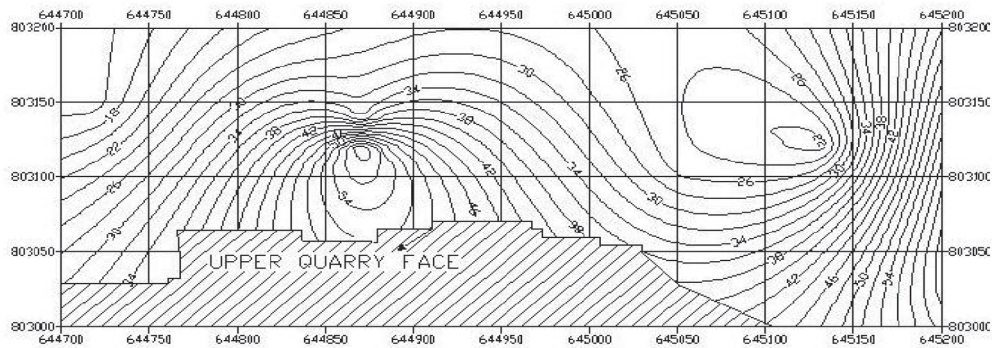

Figure 13. PPV Contour Map for the upper bench.

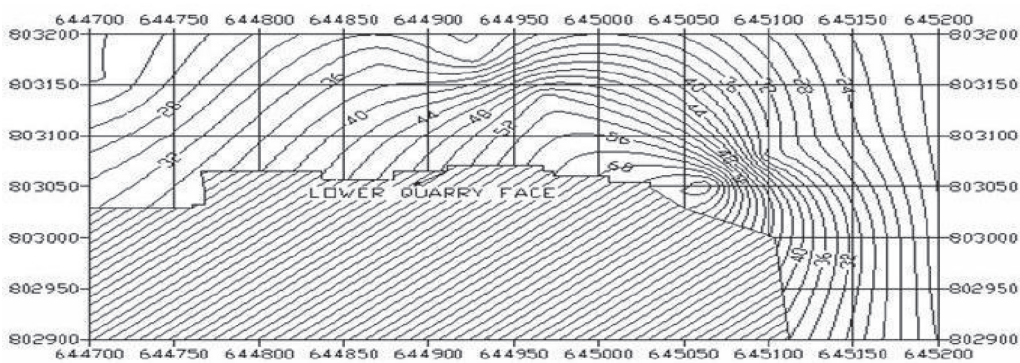

Figure 14. PPV Contour Map for the lower bench.

8. PPVCONTOUR MAPS

The above significant variations in PPV and its rate of attenuation at NE and NW directions, encouraged the authors to collect all the measured data, in order to conduct contour maps for both of upper and lower benches, at TPCC limestone quarry, as in Figures 13 & 14.

These maps help with the prediction of PPV value at any location, in case a suitable instrument is not available, as well as the attenuation rate of PPV at any profile can be easily estimated.

9. CONCLUSIONS

Authority's constraint will restrict more and more blasting works in TPCC limestone quarry. So, vibration study is of great importance for the elimination of authorities problems. From studying the attenuation rate of PPV with distance, it is concluded that:

- Near-Field, for the upper bench: - 1.15
- Near-Field, for the lower bench: - 0.32
- Far-Field, for both of upper and lower benches: - 0.003

This difference in the attenuation rates between the upper and lower benches is due to the presence of anisotropic and fissured limestone in upper bench, so its absorption of seismic energy is very high.

It is also highlighted from the distribution of PPV data that, there is no statistical significant effect of the azimuth on PPV values, which is support the heterogeneity phenomena of the limestone deposit.

By applying the concept of the scaled distance, the constants of (K) and (α) have been determined separately for the NE and NW directions, as following:

- NE direction: (K) = 1200, and (α) = 1.56
- NW direction: (K) = 208, and (α) = 1.06

It is noticed, that the NE direction yields significantly high PPV values, combined with high rate of attenuation. This means that, the PPV value was initiated high in NE than NW direction, and then abruptly decreased. In consequently, TPCC limestone concession can be extended safely in the NE direction.

All the PPV measured data were employed to conduct contour maps for both of upper and lower benches, at TPCC limestone quarry. These maps help in the prediction of the PPV values at different locations, when a suitable instrument is not available in the site, then the attenuation rate of PPV for any profile can be easily estimated.

Based on the results of this study, the presence of fissures in the upper bench, leads to increase in the attenuation rate of PPV, then the creation of an artificial fissure plane in the lower bench is recommended to increase its absorption for ground vibration.

A line of Pre-split blast is recommended to create an artificial fissure plane at the distance of 305 m, from Tourah caves, which previously calculated as the minimum safe distance. The Pre-split line forms as L-shape, where its longer arm parallel to the cave and running EW direction. While the shorter one perpendicular to the caves in the quarry direction, and running NS direction. Therefore, the ground vibrations will be absorbed in both directions.

To design the Pre-split line, a total of 169 blast hole is required, with 1.25 m hole spacing, and blasted in groups. The number of blast holes in each group will be 13 holes, initiated instantaneously, each hole fired with 14.8 kg of gelatin dynamite (cartridge), and taped with detonating cord. The cartridge length is 0.40 m, and the following 0.40 m will be left as spacing between the cartridges. Ten groups will be blasted in the longer arm, with 162.5 m length, while 2 groups will be in the shorter one, with 48.75 m length.

The blast holes of the Pre-split will be drilled from the top surface of the quarry to the full depth of both benches, while only the lower 60.0 m will be charged according to the above system. By this procedure, the Pre-split will create artificial planes in the lower bench equivalent, to large extent, to that of the upper bench.

10. ACKNOWLEDGEMENTS

The authors would express their great thanks to A. Makarem (Quarry Manager), M. Kamal (Blasting Eng.) and Kh. Korany (Surveyor) from ASEC Company for Mining (ASCOM), for their co-operation in performing these investigations.

REFERENCES

Aimone-Martin, C. 2007. Development of An Urban Blasting Ordinance for the City of Hendrson,

NV. *Vol. 1, Proc. 33rd Ann.Conf. Explosives and Blasting Tech*; ISEE.

Dowding, C.H. 1985. Blast Vibration Monitoring and control. *Prentice-Hall*, INC., NJ.

Farag, I.A.M. & Ismail, A. 1959. Contribution to the Stratigraphy of the Wadi Hof area (northeast of Helwan). *Bull. Fac. Sci.*, Cairo Univ., 34, 147-168.

Khaled, M., Abdel Rahman, K. & Makarem, A. 2007. Experimental Techniques To Reduce Blast Vibration Level, Tourah, Cairo, Egypt. *Vol. 1, Proc. 33rd Ann.Conf. Explosives and Blasting Tech; ISEE.*

Persson, P., Holmberg, R. & Lee, J. 1994. Rock blasting and Explosives Engineering. *Library of Congress, Cataloging – in- publication data, 551.*

Singh, V. & Singh, T. 2006. Safe blasting near important civil structures: A case study. *Vol. 1, Proc. 32nd Ann.Conf. Explosives and Blasting Tech; ISEE.*